

# Magneto-optical transport in type-II Weyl semimetals in the presence of orbital magnetic moment

Panchlal Prabhat

*Department of Physics, Lalit Narayan Mithila University, Darbhanga, Bihar 846004, India*

Amit Gupta

*Department of Physics, M. R. M. College, Lalit Narayan Mithila University, Darbhanga, Bihar 846004, India*

(Dated: February 5, 2026)

The magneto-optical transport of gapless type-I tilted single Weyl semimetals(WSMs) exhibits suppression of total magnetoconductivities in the presence of orbital magnetic moment(OMM) in linear and nonlinear responses (Yang Gao et al., Phys. Rev. B **105**, 165307 (2022)). In this work, we extend our study to investigate magnetoconductivities in gapless type-II Weyl semimetals within the semiclassical Boltzmann approach and show the differences that arise compared to single-Weyl semimetals.

## I. INTRODUCTION

In particle physics, Weyl fermions charge carrying, massless particles were proposed by Herman Weyl in 1929 [1]. Weyl semimetals are naturally occurring condensed matter systems that have been experimentally realized as quasi particles[2–4]. In a three-dimensional condensed matter system, the Weyl semimetals phase a topological of matter, has been found experimentally to host linear dispersion quasi particles with unique chirality[2, 5, 6]. In the Brillouin zone, the topological material manifests itself as a pair of conduction and valence bands that touch at a discrete location known as the Weyl points[6–12]. The Berry curvature in momentum space at the Weyl node with monopole indicates a nontrivial topological characteristic resulting from this special band structure, which is typically regarded as an effective magnetic field.

In any topological lattice that is invariant under the gauge field and the action is bilinear in fermionic fields, the chiral Weyl fermions always exist in pairs of opposing chirality[13]. The Weyl nodes in Weyl semimetals with broken time reversal symmetry arrive in pairs of equal energy, but their chirality is opposite and they are displaced in momentum. Additionally, the Weyl points are no longer at the same energy if inversion symmetry is broken. Several materials like TaAs, NbAs [2, 3],  $YbMnBi_2$  [14],  $HgCr_2Se_4$ [11] and Pyrochlore iridates[8] have been found to be Weyl semimetals with pairs of Weyl nodes showing opposite chirality. These materials exhibit unique properties namely negative magnetoresistance [5, 15] and surface state with Fermi arcs associated with chiral anomaly[16, 17]. They also exhibit an anomalous Hall effect[10, 18–21].

The Weyl nodes in condensed matter systems can also be anisotropic and tilted (called type-I) and tilted over (type-II)[22–29]. In type-I WSM, the tilt is supposed to be smaller than the Fermi velocity  $v_F$ . There is a closed Fermi surface enclosing either electron or a hole pocket,

with a single point consistent with Weyl node. However, in type-II WSM, the tilt becomes larger than  $v_F$ , the Fermi surface no longer just a point, at the Fermi surface there exists a unbounded electron and hole pockets and even at Weyl point, there are large density of state exist[22], which outcomes in different magnetotransport properties of type-II WSM[20, 30–34].

The Berry curvature functions as a magnetic field in the momentum space, and Weyl nodes are either a source or a sink of this curvature[35, 36]. There is a significant influence from this on the electron wavepacket dynamics in the WSM lattice, especially when there are parallel magnetic and electric fields (a finite  $\mathbf{E} \cdot \mathbf{B}$  term). This leads to a variety of intriguing magnetoconductivity (MC) and magneto-thermal transport features in WSM, which have been thoroughly studied theoretically[19, 33, 34, 37–48].

In this paper, we study the linear and nonlinear magneto-optical responses for tilted type-II WSM in the presence of an orbital magnetic moment. This has been studied for WSMs without tilt term [49] as well as type-I WSM [50]. The linear linear response has been studied for type-II WSM without OMM [51]. However, non-linear magnetoconductivity has not been discussed in the literature with the combined effects of both the tilting and orbital magnetic moment terms [52]. The orbital magnetic moment can be thought of as the self-rotation of the Bloch wave packet, and modifies the energy of the Bloch electron under the external magnetic field [53]. This orbital moment suppresses the magneto-optical responses of tilted WSM [50]. We derive an analytic expression for the magnetoconductivity employing the semiclassical Boltzmann approach. It is found that the orbital magnetic moment induces a non-trivial magnetoconductivity term, which gives rise to a partial cancellation of the total magnetoconductivity. This cancellation are more pronounced compared to type-I WSMs. This cancellation is more pronounced compared to isotropic WSMs. Further, we analyzed this suppressed

feature for linear and quadratic contributions in the magnetic field to magnetoconductivities. We also show that the linear-B (quadratic-B) magnetoconductivity exhibits a behavior that is dependent (independent) of the chirality of the Weyl node in both linear or nonlinear response regimes, as in the case of type-I WSMs[50].

The paper is organized as follows: In Sec.II, we begin with the model of a tilted-Weyl semimetal with a tilt in the  $z$  direction, and then the semiclassical equations of motion for the dynamics of the electron wave packet in the electric and magnetic fields are presented. We have reproduced the results and figures for type-I WSMs to compare with its type-II WSMs. In Sec. III, the B-linear and quadratic-B magnetoconductivities including the orbital magnetic moment are obtained in the linear response regime, and analyzed in detail. In Sec. IV, we study second harmonic generation, and give the second harmonic conductivity formula as well as the further analysis for this result. We end with conclusions in Sec. V.

## II. MODEL HAMILTONIAN AND SEMICLASSICAL BOLTZMANN APPROACH

The non-interacting low-energy effective Hamiltonian for tilted Weyl semimetals is given by [20],

$$\mathcal{H}_0 = s\hbar v_F \mathbf{k} \cdot \boldsymbol{\sigma} + \hbar v_F t_s k_z \sigma_0 \quad (1)$$

where  $s = \pm 1$  is the chirality of the Weyl node,  $\mathbf{k}$  is the momentum,  $v_F$  is the effective velocity along the direction of  $\hat{z}$ ,  $\boldsymbol{\sigma}\{\sigma_x, \sigma_y, \sigma_z\}$  and  $\sigma_0$  is a identity matrix  $2 \times 2$ . The energy dispersion for WSMs is given by  $\epsilon_{\mathbf{k}}^s = \hbar t_s v_F k_z \pm \hbar v_F k$  with  $\pm$  represent for the conduction and valence bands respectively. This Hamiltonian corresponds to type-I WSM only for small tilt parameter  $t_s < 1$ , such that the Fermi surface encloses only a electron ( $\mu > 0$ ) or a hole ( $\mu < 0$ ) pocket. And for type-II WSM, tilt parameter  $t_s > 1$ , leading over tilted WNs and at the Fermi energy, the presence of unbounded electron and hole pockets. In type-II WSM, there is finite contibution from both the Valence and conduction bands to all physical properties, which is contrast to type-I WSM. We will use semiclassical Boltzmann equations in this study.

In the presence of a static magnetic field  $\mathbf{B}$  and a time varying electric field  $\mathbf{E}$ , the semiclassical equations of motion at the location  $\mathbf{r}$  and the wave-vector  $\mathbf{k}$  in a given band are [36, 53]

$$\dot{\mathbf{r}} = \frac{1}{\hbar} \nabla_{\mathbf{k}} \tilde{\epsilon}_{\mathbf{k}}^s - \dot{\mathbf{k}} \times \Omega_{\mathbf{k}}^s \quad (2)$$

$$\hbar \dot{\mathbf{k}} = -e\mathbf{E} - e\dot{\mathbf{r}} \times \mathbf{B} \quad (3)$$

where  $-e$  is the electron charge. The first term on the right-hand side of Eq. (2) is  $\mathbf{v}_{\mathbf{k}}^s = \frac{1}{\hbar} \nabla_{\mathbf{k}} \tilde{\epsilon}_{\mathbf{k}}^s$ , defined in

terms of an effective band dispersion  $\tilde{\epsilon}_s(\mathbf{k})$ . In topological metals such as WSMs, this quantity acquires a term due to the intrinsic orbital moment,i.e.,  $\tilde{\epsilon}_{\mathbf{k}}^s = \epsilon_{\mathbf{k}}^s - \mathbf{m}_{\mathbf{k}}^s \cdot \mathbf{B}$ , while  $\mathbf{m}_{\mathbf{k}}^s$  is the orbital moment induced by the semiclassical “self-rotation” of the Bloch wave packet. The term  $\Omega_{\mathbf{k}}^s$  is the Berry curvature [36, 53]

$$\Omega_{\mathbf{k}}^s = Im[\langle \nabla_{\mathbf{k}} u_{\mathbf{k}}^s | \times | \nabla_{\mathbf{k}} u_{\mathbf{k}}^s \rangle] \quad (4)$$

$$\mathbf{m}_{\mathbf{k}}^s = -\frac{e}{2\hbar} Im[\langle \nabla_{\mathbf{k}} u_{\mathbf{k}}^s | \times (\mathcal{H}_J(\mathbf{k}) - \epsilon_{\mathbf{k}}^s) | \nabla_{\mathbf{k}} u_{\mathbf{k}}^s \rangle] \quad (5)$$

where  $|u_{\mathbf{k}}^s\rangle$  satisfies the equation  $\mathcal{H}_0(\mathbf{k})|u_{\mathbf{k}}^s\rangle = \epsilon_{\mathbf{k}}^s |u_{\mathbf{k}}^s\rangle$ .

The general expressions for Berry curvature and orbital magnetic moment for WSMs are [54]

$$\Omega_{\mathbf{k}}^s = -s \frac{(k_x, k_y, k_z)}{2k^3} \quad (6)$$

$$\mathbf{m}_{\mathbf{k}}^s = -s \frac{ev_F(k_x, k_y, k_z)}{2k^2} \quad (7)$$

The two equations (2) and (3) can be decoupled to get

$$\dot{\mathbf{r}} = \frac{1}{\hbar D} [\nabla_{\mathbf{k}} \tilde{\epsilon}_{\mathbf{k}}^s + e\mathbf{E} \times \Omega_{\mathbf{k}}^s] + \frac{e}{\hbar} (\nabla_{\mathbf{k}} \tilde{\epsilon}_{\mathbf{k}}^s \cdot \Omega_{\mathbf{k}}^s) \mathbf{B} \quad (8)$$

$$\hbar \dot{\mathbf{k}} = \frac{1}{\hbar D} [-e\mathbf{E} - \frac{e}{\hbar} \nabla_{\mathbf{k}} \tilde{\epsilon}_{\mathbf{k}}^s \times \mathbf{B} - \frac{e^2}{\hbar} (\mathbf{E} \cdot \mathbf{B}) \Omega_{\mathbf{k}}^s] \quad (9)$$

where the factor  $D = 1 + \frac{e}{\hbar} (\Omega_{\mathbf{k}}^s \cdot \mathbf{B})$  modifies the phase space volume [55].

For a given chirality  $s = \pm$  of a single Weyl node, the semiclassical Boltzmann equation (SBE) reads as follows

$$\frac{\partial \tilde{f}^s}{\partial t} + \dot{\mathbf{k}} \cdot \frac{\partial \tilde{f}^s}{\partial \mathbf{k}} = \frac{\tilde{f}^s - \tilde{f}_0^s}{\tau} \quad (10)$$

Here,  $\tilde{f}^s(\tilde{\epsilon}_{\mathbf{k}}^s)$  is the electron distribution function. where  $\tau$  is the relaxation time originating from the scattering of electrons by phonons, impurities, electrons, and other lattice imperfections [56].

The  $\tilde{f}_0^s(\tilde{\epsilon}_{\mathbf{k}}^s)$  can be expanded at low magnetic field as [57]

$$\begin{aligned} \tilde{f}_0^s(\tilde{\epsilon}_{\mathbf{k}}^s) &= \tilde{f}_0^s(\epsilon_{\mathbf{k}}^s - \mathbf{m}_{\mathbf{k}}^s \cdot \mathbf{B}) \\ &\approx \tilde{f}_0^s(\epsilon_{\mathbf{k}}^s) - \mathbf{m}_{\mathbf{k}}^s \cdot \mathbf{B} \frac{\partial \tilde{f}_0^s(\epsilon_{\mathbf{k}}^s)}{\partial \epsilon_{\mathbf{k}}^s} \end{aligned} \quad (11)$$

where  $\tilde{f}_0^s(\epsilon_{\mathbf{k}}^s) = 1/[e^{(\epsilon_{\mathbf{k}}^s - \mu)/k_B T} + 1]$  with  $k_B$  the Boltzmann constant, T the temperature, and  $\mu$  the chemical potential.

Eq.(10) can be solved by expanding the distribution function as a power series in the electric field as

$$\tilde{f}^s = \tilde{f}_0^s + \tilde{f}_1^s e^{-i\omega t} + \tilde{f}_2^s e^{-2i\omega t} + \dots \quad (12)$$

where  $\tilde{f}_1^s$  and  $\tilde{f}_2^s$  are the first- and second-order terms for  $\mathbf{E}$ , respectively. The electric current density can be calculated by

$$\mathbf{j} = -\frac{e}{(2\pi)^3} \int d^3k D\mathbf{r} \tilde{f}^s \quad (13)$$

Equation(13) compute the conductivity components under the combined influence of external electric and magnetic fields.

### III. LINEAR RESPONSE OF TILTED WSMS

For linear electric field response, we retain only the first two terms of Eq.(12) and substitute Eq.(8) in Eq.(10)

$$\frac{1}{\hbar D} [-e\mathbf{E} - \frac{e^2}{\hbar} (\mathbf{E} \cdot \mathbf{B}) \Omega_{\mathbf{k}}^s] \cdot \frac{\partial \tilde{f}_0^s}{\partial \mathbf{k}} - i\omega \tilde{f}_1^s = -\frac{\tilde{f}_1^s}{\tau} \quad (14)$$

Solved for  $\tilde{f}_1^s$ , we obtain

$$\tilde{f}_1^s = \frac{\tau}{(1 - i\omega\tau)} \frac{1}{\hbar D} [e\mathbf{E} + \frac{e^2}{\hbar} (\mathbf{E} \cdot \mathbf{B}) \Omega_{\mathbf{k}}^s] \cdot \frac{\partial \tilde{f}_0^s}{\partial \mathbf{k}} \quad (15)$$

We expand Eq.(15) up to the second order in magnetic field and obtain

$$\begin{aligned} \tilde{f}_1^s = & \frac{\tau}{(1 - i\omega\tau)} \left[ e\mathbf{E} \cdot \mathbf{v}_{\mathbf{k}}^s \cdot \frac{\partial \tilde{f}_0^s}{\partial \epsilon_{\mathbf{k}}^s} - \frac{e^2}{\hbar} (\mathbf{B} \cdot \Omega_{\mathbf{k}}^s) (\mathbf{E} \cdot \mathbf{v}_{\mathbf{k}}^s) \frac{\partial \tilde{f}_0^s}{\partial \epsilon_{\mathbf{k}}^s} + \frac{e^2}{\hbar} (\mathbf{E} \cdot \mathbf{B}) (\Omega_{\mathbf{k}}^s \cdot \mathbf{v}_{\mathbf{k}}^s) \frac{\partial \tilde{f}_0^s}{\partial \epsilon_{\mathbf{k}}^s} - \frac{e}{\hbar} \mathbf{E} \cdot \frac{\partial}{\partial \mathbf{k}} \left( \mathbf{m}_{\mathbf{k}}^s \cdot \mathbf{B} \frac{\partial \tilde{f}_0^s}{\partial \epsilon_{\mathbf{k}}^s} \right) \right. \\ & - \frac{e^3}{\hbar^2} (\mathbf{B} \cdot \Omega_{\mathbf{k}}^s) (\mathbf{E} \cdot \mathbf{B}) (\Omega_{\mathbf{k}}^s \cdot \mathbf{v}_{\mathbf{k}}^s) \frac{\partial \tilde{f}_0^s}{\partial \epsilon_{\mathbf{k}}^s} + \frac{e^3}{\hbar^2} (\mathbf{B} \cdot \Omega_{\mathbf{k}}^s)^2 (\mathbf{E} \cdot \mathbf{v}_{\mathbf{k}}^s) \frac{\partial \tilde{f}_0^s}{\partial \epsilon_{\mathbf{k}}^s} + \frac{e^2}{\hbar^2} (\mathbf{B} \cdot \Omega_{\mathbf{k}}^s) \mathbf{E} \cdot \frac{\partial}{\partial \mathbf{k}} \left( \mathbf{m}_{\mathbf{k}}^s \cdot \mathbf{B} \frac{\partial \tilde{f}_0^s}{\partial \epsilon_{\mathbf{k}}^s} \right) \\ & \left. - \frac{e^2}{\hbar^2} \Omega_{\mathbf{k}}^s \cdot \frac{\partial}{\partial \mathbf{k}} \left( \mathbf{m}_{\mathbf{k}}^s \cdot \mathbf{B} \frac{\partial \tilde{f}_0^s}{\partial \epsilon_{\mathbf{k}}^s} \right) \right] \end{aligned} \quad (16)$$

From Eqs.(8) and Eq.(16), the expression for current density at time  $t$  is given by

$$\begin{aligned} \mathbf{j}_1 = & -\frac{e}{(2\pi)^3} \int d^3k \left[ \tilde{\mathbf{v}}_{\mathbf{k}}^s + \frac{e}{\hbar} (\Omega_{\mathbf{k}}^s \cdot \tilde{\mathbf{v}}_{\mathbf{k}}^s) \mathbf{B} \right] \tilde{f}_1^s \\ & - \frac{e^2}{2\pi)^3 \hbar} \int d^3k \mathbf{E} \times \Omega_{\mathbf{k}}^s \tilde{f}_0^s \end{aligned} \quad (17)$$

The above equation can be expressed in frequency space  $\omega$  as

$$j_a(\omega) = \sigma_{ab}(\omega) E_b(\omega) \quad (18)$$

where  $\sigma_{ab}(\omega)$  is the frequency dependent conductivity. It is known that the single contribution from the group velocity  $\tilde{\mathbf{v}}_{\mathbf{k}}^s$  or the Berry curvature  $\Omega_{\mathbf{k}}^s$  form the conventional longitudinal or Hall conductivities. In the presence of the magnetic field, the conductivity  $\sigma(\omega)$  consists of

the coupling terms between the group velocity  $\tilde{\mathbf{v}}_{\mathbf{k}}^s$  and the Berry curvature  $\Omega_{\mathbf{k}}^s$  besides the conventional ingredients [see Eq. (17)]. Their combined contributions are triggered by the external magnetic field, and play a crucial role in the electron transport.

#### A. Calculations of longitudinal conductivities components without magnetic field

Substituting Eq.(16) without  $\mathbf{B}$  terms into the first term of Eq.(17), we get longitudinal conductivities components

$$\sigma_{ab}^{(0)}(\omega) = \frac{\tau}{(1 - i\omega\tau)} \frac{e^2}{(2\pi)^3} \int d^3k v_a^s v_b^s \left( -\frac{\partial f_0^s}{\partial \epsilon_{\mathbf{k}}^s} \right) \quad (19)$$

$$\sigma_{zz}^0(\omega) = \frac{3\sigma_D}{2t_s^3} \left[ -2t_s - \ln \frac{1 - t_s}{1 + t_s} \right] \quad (20)$$

$$\sigma_{xx}^0(\omega) = \sigma_{yy}^0(\omega) = \frac{3\sigma_D}{4t_s^3} \left[ \frac{2t_s}{(1 - t_s^2)} + \ln \frac{1 - t_s}{1 + t_s} \right] \quad (21)$$

At  $T=0$  K,  $-\frac{\partial f_0^s}{\partial \epsilon_{\mathbf{k}}^s} = \delta(\epsilon_{\mathbf{k}}^s - \mu)$ , we get

For type-I,

For type-II,

$$\sigma_{zz}^0(\omega) = \frac{3\sigma_D}{2t_s^3} \left[ 3 - t_s^2 + (t_s^2 - 1)^2 \tilde{\Lambda}_k^2 + \ln(t_s^2 - 1) + 2 \ln \tilde{\Lambda}_k \right] \quad (22)$$

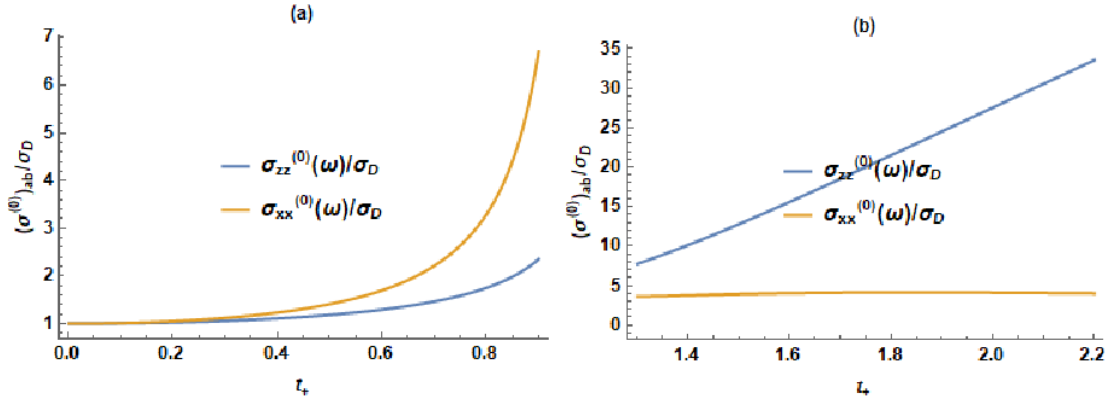


FIG. 1. The dependence of the optical conductivity on the tilt  $t_+$  at zero B field for (a) type-I WSM and (b) type-II WSM. The other parameters are taken as  $\tilde{\Lambda}_k = 4$ ,  $v_F = 4.13 \times 10^5$  m / s,  $\mu = 1$  meV, and  $\tau = 10^{-13}$  s.

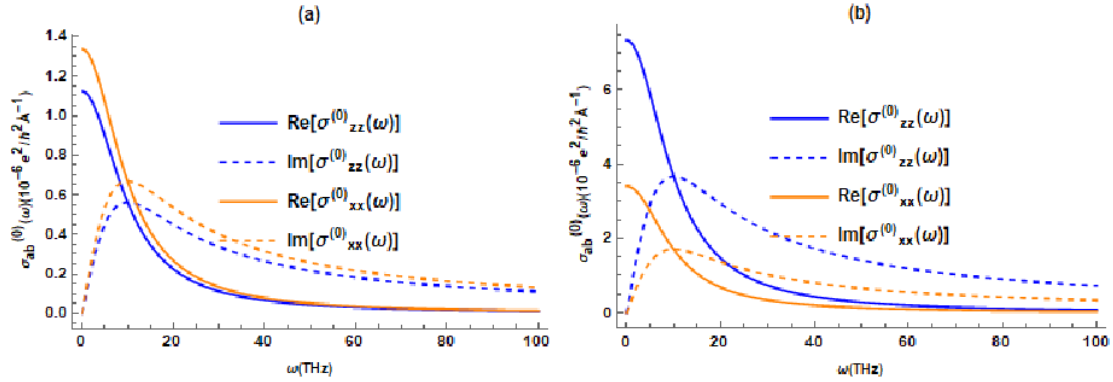


FIG. 2. The frequency dependence of optical conductivity at zero B-field for (a) type-I WSM at  $t_s = 0.5$  and (b) type-II WSM at  $t_s = 1.3$ . The other parameters are the same as those of Fig. (1)

$$\sigma_{xx}^0(\omega) = \frac{3\sigma_D}{4t_s^3} \left[ \frac{3-t_s^2}{t_s^2-1} + (t_s^2-1)\tilde{\Lambda}_k^2 - \ln(t_s^2-1) - 2\ln\tilde{\Lambda}_k \right] \quad (23)$$

where  $\sigma_D = \frac{e^2\tau\mu^2}{(1-i\omega\tau)6\pi^2\hbar^3v_F}$  is Drude frequency complex

conductivity. Unlike the case of type-I WSM [Fig. 1(a)], for a type-II WSM we find that  $\sigma_{zz}(0)$  is larger and more sensitive to  $t_s$  as compared to  $\sigma_{xx}(0)$  [Fig. 1(b)] [51]. The frequency dependence of conductivity components are shown in Fig. 2.

## B. Calculations of conductivities components linear in magnetic field

Substituting Eq.(16) with  $\mathbf{B}$  terms up to first order into the first term of Eq.(17), we get conductivities com-

ponents

$$\sigma_{ab}^{(B)}(\omega) = \sigma_{ab}^{(B,\Omega)}(\omega) + \sigma_{ab}^{(B,m)}(\omega) \quad (24)$$

where

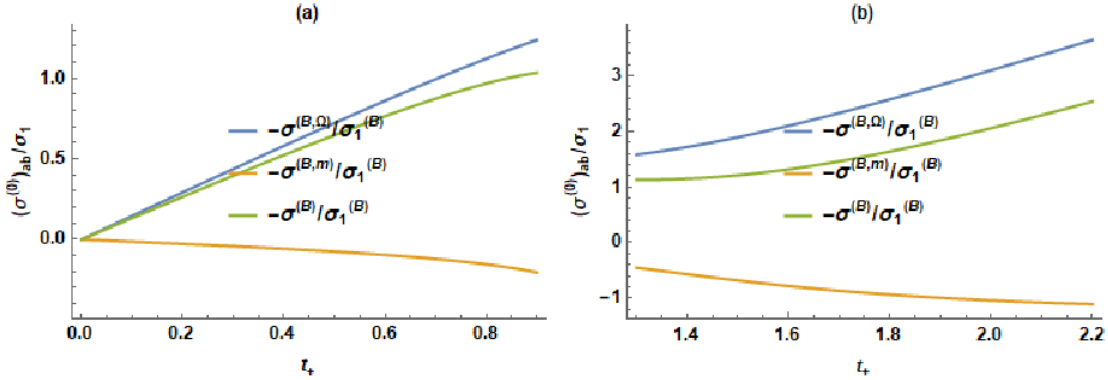


FIG. 3. The dependence of the optical conductivity at  $B=1$  on the tilt  $t_+$  for (a) type-I WSM and (b) type-II WSM. The other parameters are the same as those of Fig.(1)

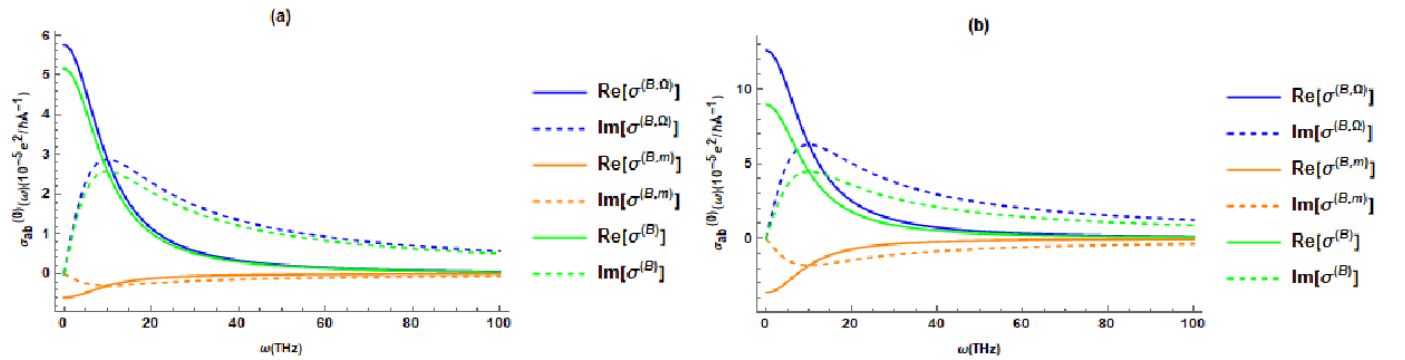


FIG. 4. The frequency dependence of optical conductivity at  $B = 1$  T for (a) type-I WSM at  $t_s = 0.5$  and (b) type-II WSM at  $t_s = 1.3$ . The other parameters are the same as those of Fig.(1)

$$\sigma_{ab}^{(B,\Omega)}(\omega) = \frac{\tau}{\hbar(1-i\omega\tau)} \frac{e^3}{(2\pi)^3} \int d^3k [(v_a^s B_b + v_b^s B_a)(\Omega_k^s \cdot \mathbf{v}_k^s) - v_a^s v_b^s (\Omega_k^s \cdot \mathbf{B})] \left( -\frac{\partial f_0^s}{\partial \epsilon_k^s} \right) \quad (25)$$

$$\sigma_{ab}^{(B,m)}(\omega) = \frac{\tau}{\hbar(1-i\omega\tau)} \frac{e^2}{(2\pi)^3} \int d^3k \left[ \frac{\partial v_a^s}{\partial k_b} (\mathbf{m}_k^s \cdot \mathbf{B}) - \frac{\partial (\mathbf{m}_k^s \cdot \mathbf{B})}{\partial k_a} v_b^s \right] \left( -\frac{\partial f_0^s}{\partial \epsilon_k^s} \right) \quad (26)$$

We can easily check from Eqs.(25) and (26) that  $\sigma_{ab}^{(B)}(\omega) = \sigma_{ba}^{(B)}(\omega)$ . The system possesses the time-reversal symmetry without tilt term and therefore conductivities will vanish [49, 50]. However, the time-reversal symmetry is broken for a finite value of tilt  $t_s \neq 0$ . The first term and the second term in Eq. (25) is related to the Berry curvature  $\Omega$  and the orbital magnetic moment respectively and has been studied in details for isotropic WSMs [50]. In the following, the detailed analysis of Eq. (25) is given by considering the magnetic field  $\mathbf{B}$  perpendicular and parallel to the tilt direction  $t_s$ .

### Case-I When $\mathbf{B} \parallel \hat{\mathbf{t}}_s \parallel \hat{\mathbf{z}}$

In this case, Hall conductivities components are zero, and one can get the following expressions for longitudinal components.

For Type-I

$$\sigma_{zz}^{(B,\Omega)} = \sigma_1^{(B)} s \left[ \frac{2(3 - 5t_s^2 - 3t_s^4)}{3t_s^3} + \frac{(t_s^2 - 1)^2}{t_s^4} \ln \left( \frac{1 - t_s}{1 + t_s} \right) \right] \quad (27)$$

$$\sigma_{xx}^{(B,\Omega)} = \sigma_1^{(B)} s \left[ \frac{2t_s^2 - 3}{3t_s^3} - \frac{1 - t_s^2}{2t_s^4} \ln \left( \frac{1 - t_s}{1 + t_s} \right) \right] \quad (28)$$

for Type-II

$$\begin{aligned}\sigma_{zz}^{(B,\Omega)} &= \frac{\sigma_1^{(B)} s}{6\pi t_s^4} \left[ 2 \left\{ \tilde{\Lambda}_k^{-3} - 3(-3 + t_s^2) \tilde{\Lambda}_k + 3k_F(3 - 4t_s^2 + t_s^4) \Lambda_k^2 + \{11 + t_s(-3 + t_s(-18 + t_s(5 - 3(-1 + t_s)t_s)))\} \right\} \right. \\ &\quad \left. - 3(-1 + t_s^2)^2 \{3 \ln[-1 + t_s] + \ln[1 + t_s] + 4 \ln \tilde{\Lambda}_k\} \right] \end{aligned}\quad (29)$$

$$\sigma_{xx}^{(B,\Omega)} = \frac{\sigma_1^{(B)} s}{6t_s^4} \left[ 2 \left\{ \tilde{\Lambda}_k^{-3} - 3(-3 + t_s^2) \tilde{\Lambda}_k^{-1} + t_s(-3 + 2t_s^2) \right\} - 3(-1 + t_s^2) \ln \left( \frac{t_s - 1}{t_s + 1} \right) \right] \quad (30)$$

Via the similar calculation, Eq.(26) becomes

for Type-I

$$\sigma_{zz}^{(B,m)}(\omega) = \sigma_1^{(B)} s \left[ \frac{2(-3 + 5t_s^2)}{3t_s^3} - \frac{(t_s^2 - 1)^2}{t_s^4} \ln \frac{1 - t_s}{1 + t_s} \right] \quad (31)$$

$$\sigma_{xx}^{(B,m)}(\omega) = \sigma_1^{(B)} s \left[ \frac{(3 - 8t_s^2)}{3t_s^3} - \frac{1 - 3t_s}{2t_s^4} \ln \frac{1 - t_s}{1 + t_s} \right] \quad (32)$$

for Type-II

$$\sigma_{zz}^{(B,m)}(\omega) = \frac{\sigma_1^{(B)} s}{6\pi t_s^4} \left[ \tilde{\Lambda}_k^{-2}(-9 + 6t_s^2) + (-11 + 21t_s^2 - 6t_s^4) - 3(-1 + t_s^2)^2 \left\{ \ln(t_s^2 - 1) - 2 \ln \tilde{\Lambda}_k \right\} \right] \quad (33)$$

$$\begin{aligned}\sigma_{xx}^{(B,m)}(\omega) &= \frac{\sigma_1^{(B)} s}{12t_s^4} \left[ 2\tilde{\Lambda}_k^{-3} + 3(3 + t_s)\tilde{\Lambda}_k^{-2} - 6\{ -3 + t_s(2 + 3t_s) \} \tilde{\Lambda}_k^{-1} + \{11 + t_s(3 + t_s(-15 + 13t_s))\} \right. \\ &\quad \left. + 6(-1 + 3t_s^2) \{ \ln[(-1 + t_s)\tilde{\Lambda}_k] + t_s \ln[(1 + t_s)\tilde{\Lambda}_k] \} \right] \end{aligned}\quad (34)$$

where  $\sigma_1^{(B)} = \frac{e^3 \tau B v_F}{(1 - i\omega\tau)8\pi^2\hbar^2}$ . From Eq.(27)-(33) unlike the case of type-I WSM, there is Fermi energy dependence that is tied to the cutoff. The total linear-B contribution of two nodes having parallel tilt becomes zero as in the type-I case. But, for nodes having opposite tilt, as is usually the case, the total contribution is nonzero.

Case-II For  $\mathbf{B} \perp \hat{\mathbf{t}}_s (\parallel \hat{\mathbf{z}})$

We can represent the magnetic field in the x-y plane as  $\mathbf{B} = B(\hat{i} \cos \gamma + \hat{j} \sin \gamma)$  where  $\gamma$  is the angle between

magnetic field  $\mathbf{B}$  and x-axis. In this case, longitudinal components of conductivities are zero and we get the following expressions for planer Hall conductivities [50, 51]

$$\sigma_{xz}^{(B)}(\omega) = [\sigma^{(B,\Omega)}(\omega) + \sigma^{(B,m)}(\omega)] \cos \theta \quad (35)$$

$$\sigma_{yz}^{(B)}(\omega) = [\sigma^{(B,\Omega)}(\omega) + \sigma^{(B,m)}(\omega)] \sin \theta \quad (36)$$

$$\sigma_{xz}^{(B,\Omega)}(\omega) = \frac{\tau}{\hbar(1 - i\omega\tau)} \frac{e^3}{(2\pi)^3} \int d^3k [v_z^s B \cos \gamma (v_x^s \Omega_{ky} + v_z^s \Omega_{kz}) - v_z^s B \sin \gamma v_x^s \Omega_{ky}] \left( -\frac{\partial f_0^s}{\partial \epsilon_{\mathbf{k}}^s} \right) \quad (37)$$

$$\sigma_{xz}^{(B,m)}(\omega) = \frac{\tau}{\hbar(1 - i\omega\tau)} \frac{e^2}{(2\pi)^3} \int d^3k \left[ B \cos \theta \left( \frac{\partial v_x^s}{\partial k_z} m_{kx}^s - v_z^s \frac{\partial m_{kx}^s}{\partial k_z} \right) - B \sin \theta \left( \frac{\partial v_x^s}{\partial k_z} m_{ky}^s - v_z^s \frac{\partial m_{ky}^s}{\partial k_x} \right) \right] \left( -\frac{\partial f_0^s}{\partial \epsilon_{\mathbf{k}}^s} \right) \quad (38)$$

The second term of both the above equations contributes

to zero.

for Type-I

$$\sigma^{(B,\Omega)} = \sigma_1^{(B)} s \left[ \frac{-3 + 5t_s^2 - 6t_s^4}{3t_s^3} - \frac{(1-t_s^2)^2}{2t_s^4} \ln \frac{1-t_s}{1+t_s} \right] \quad (39)$$

$$\sigma^{(B,m)} = \sigma_1^{(B)} s \left[ -\frac{2t_s^2 - 3}{3t_s^3} + \frac{1-t_s^2}{2t_s^4} \ln \frac{1-t_s}{1+t_s} \right] \quad (40)$$

for Type-II

$$\begin{aligned} \sigma^{(B,\Omega)} = & \frac{\sigma_1^{(B)} s}{6t_s^4} \left[ 4\tilde{\Lambda}_k^{-3} - 3(-3+t_s^2)\tilde{\Lambda}_k^{-2} + 12(3-4t_s^2+t_s^4)\tilde{\Lambda}_k^{-1} - (1+t_s)\{ -11 + t_s(23 + t_s(-5 + 3t_s(-5 + 4t_s))) \} \right. \\ & \left. + 3(-1+t_s^2)^2 \left\{ \ln[(1+t_s)\tilde{\Lambda}_k] - 3\ln[(-1+t_s)\tilde{\Lambda}_k] \right\} \right] \end{aligned} \quad (41)$$

$$\begin{aligned} \sigma^{(B,m)} = & \frac{\sigma_1^{(B)} s}{6t_s^4} \left[ 2\{ \tilde{\Lambda}_k^{-3} - 3(-3+t_s^2)\tilde{\Lambda}_k^{-2} - 3k_F(-3+t_s^2)\tilde{\Lambda}_k^{-1} + \{ 11 + t_s(-3 + t_s(-12 + t_s(2 + 3t_s))) \} \} \right. \\ & \left. + 3\{ (-1+t_s^2)\{ 3\ln[(-1+t_s)\tilde{\Lambda}_k] + \ln[(1+t_s)\tilde{\Lambda}_k] \} \} \right] \end{aligned} \quad (42)$$

From Eqs.(27) to (42), we notice that the B-linear magnetoconductivity in type-I/II-Weyl semimetals is independent/dependent of Fermi energy that the tied to the cut off and the odd function of  $t_s$  [50]. According to the Nielsen-Ninomiya theorem [58], the Weyl nodes with opposite chirality always appears in pairs. The total magnetoconductivity of the system is the sum of all the Weyl nodes. Therefore, for the case of  $t_+ = t_-$ , where the tilt inversion symmetry is broken, the contribution of the Weyl node to the magnetoconductivity has the opposite sign for the opposite (B) chirality, giving rise to  $\sigma_{ab}(\omega) = 0$ . Whereas, for the case of  $t_+ = -t_-$ , where the tilt inversion symmetry is unbroken, each Weyl node produces an identical contribution to the magnetoconductivity, and so the nonzero magnetoconductivity emerges for this case. Fig.(3) and (4) show the tilt and frequency variations of linear B longitudinal

conductivity components for type-I and type-II WSMs. In case of type-II WSMs, the conductivity contribution due to Berry curvature and OMM are more pronounced compared to its type-I one. The suppressin also takes place in type-II WSM as occured in type-I.

### C. Calculations of quadratic-B contribution to the conductivity $\sigma_{ab}^{(B^2)}$

Substituting Eq.(16) with  $\mathbf{B}$  terms up to second order into the first term of Eq.(17), we get conductivities components

$$\sigma_{ab}^{(B^2)}(\omega) = \sigma_{ab}^{(B^2,\Omega)}(\omega) + \sigma_{ab}^{(B^2,m)}(\omega) \quad (43)$$

where

$$\begin{aligned} \sigma_{ab}^{(B^2,\Omega)}(\omega) = & \frac{\tau}{\hbar^2(1-i\omega\tau)} \frac{e^4}{(2\pi)^3} \int d^3k [v_a^s v_b^s (\Omega_{\mathbf{k}}^s \cdot \mathbf{B})^2 - (v_a^s B_b + v_b^s B_a) (\Omega_{\mathbf{k}}^s \cdot \mathbf{v}_{\mathbf{k}}^s) (\Omega_{\mathbf{k}}^s \cdot \mathbf{B}) \\ & + B_a B_b (\Omega_{\mathbf{k}}^s \cdot \mathbf{v}_{\mathbf{k}}^s)^2] \left( -\frac{\partial f_0^s}{\partial \epsilon_{\mathbf{k}}^s} \right) \end{aligned} \quad (44)$$

$$\begin{aligned} \sigma_{ab}^{(B^2,m)}(\omega) = & \frac{\tau}{\hbar^2(1-i\omega\tau)} \frac{e^3}{(2\pi)^3} \int d^3k \left[ \frac{\partial}{\partial \mathbf{k}} \cdot [v_a^s B_b \Omega_{\mathbf{k}}^s] (\mathbf{m}_{\mathbf{k}}^s \cdot \mathbf{B}) - \frac{\partial [v_a^s (\Omega_{\mathbf{k}}^s \cdot \mathbf{B})]}{\partial k_b} (\mathbf{m}_{\mathbf{k}}^s \cdot \mathbf{B}) + \frac{\partial [B_a^s (\Omega_{\mathbf{k}}^s \cdot v_{\mathbf{k}}^s)]}{\partial k_b} (\mathbf{m}_{\mathbf{k}}^s \cdot \mathbf{B}) + \right. \\ & \left. \frac{\partial (\mathbf{m}_{\mathbf{k}}^s \cdot \mathbf{B})}{\partial k_a} (\Omega_{\mathbf{k}}^s \cdot \mathbf{B}) v_b^s - \frac{\partial (\mathbf{m}_{\mathbf{k}}^s \cdot \mathbf{B})}{\partial k_a} (\Omega_{\mathbf{k}}^s \cdot v_{\mathbf{k}}^s) B_b^s - \frac{\partial^2 (\mathbf{m}_{\mathbf{k}}^s \cdot \mathbf{B})}{\epsilon \partial k_a \partial k_b} (\mathbf{m}_{\mathbf{k}}^s \cdot \mathbf{B}) - B_a \frac{\partial (\mathbf{m}_{\mathbf{k}}^s \cdot \mathbf{B})}{\partial \mathbf{k}} \cdot \Omega_{\mathbf{k}}^s v_b^s \right] \left( -\frac{\partial f_0^s}{\partial \epsilon_{\mathbf{k}}^s} \right) \end{aligned} \quad (45)$$

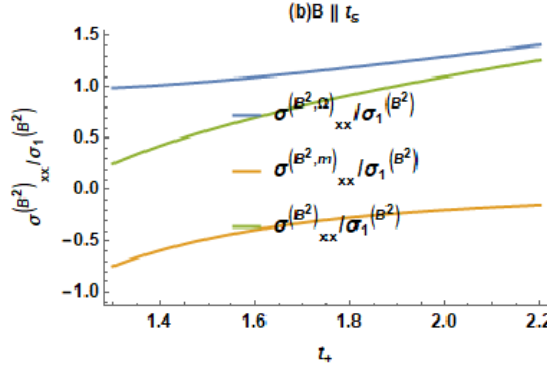


FIG. 5. The dependence of the optical conductivity on the tilt  $t_+$  for the case of  $B \parallel t_s$ , for type-II WSM. The other parameters are the same as those of Fig.(1)

$\sigma_{ab}^{(B^2, \Omega)}(\omega)$  and  $\sigma_{ab}^{(B^2, m)}(\omega)$  Berry-curvature  $\Omega_k^s$  and the orbital magnetic moment  $\mathbf{m}_k^s$  dependent conductivities respectively. Consider the following two cases

components  
for Type-I

$$\sigma_{zz}^{(B^2, \Omega)}(\omega) = 8\sigma_1^{(B^2)} \quad (46)$$

Case-I When  $\mathbf{B} \parallel t_s \parallel z$

In this case, Hall conductivities components are zero and one can get the following expressions for longitudinal

$$\sigma_{xx}^{(B^2, \Omega)}(\omega) = \sigma_1^{(B^2)} \quad (47)$$

for Type-II

$$\sigma_{zz}^{(B^2, \Omega)}(\omega) = \frac{\sigma_1^{(B^2)}}{2t_s^5} \left[ -5\tilde{\Lambda}_k^{-6} + 15(-3 + t_s^2)\tilde{\Lambda}_k^{-4} - 15(-1 + t_s^2)^2\tilde{\Lambda}_k^{-2} + \left\{ 1 + 5t_s^2(-1 + 3t_s^2 + t_s^4) \right\} \right] \quad (48)$$

$$\sigma_{xx}^{(B^2, \Omega)}(\omega) = \frac{\sigma_1^{(B^2)}}{t_s^5} \left[ -6\tilde{\Lambda}_k^{-5} + 5(-2 + t_s^2)\tilde{\Lambda}_k^{-3} + t_s^5 \right] \quad (49)$$

Considering the effect of the orbital magnetic moment, we have

for Type-I

$$\sigma_{zz}^{(B^2, m)}(\omega) = (-3 + 5t_s^2)\sigma_1^{(B^2)} \quad (50) \quad \text{for Type-II}$$

$$\sigma_{xx}^{(B^2, m)}(\omega) = -\sigma_1^{(B^2)} \quad (51)$$

$$\begin{aligned} \sigma_{zz}^{(B^2, m)}(\omega) = & \frac{\sigma_1^{(B^2)}}{4t_s^5} \left[ 60\tilde{\Lambda}_k^{-6} + 15(36 - 5t_s^5)\tilde{\Lambda}_k^{-2} - 20t_s^2(-2 + t_s^2)\tilde{\Lambda}_k^{-3} + 30(6 - 5t_s^2 + t_s^4)\tilde{\Lambda}_k^{-2} \right. \\ & \left. + \left\{ -12 + 5t_s^2 \left\{ 5 + t_s^2(-6 + t_s(4 + t_s(-3 + 4t_s))) \right\} \right\} \right] \end{aligned} \quad (52)$$

$$\sigma_{xx}^{(B^2, m)}(\omega) = \frac{\sigma_1^{(B^2)}}{2t_s^5} \left[ -15\tilde{\Lambda}_F^{-6} + 15(-9 + t_s^2)\tilde{\Lambda}_k^{-4} + 15(-3 + 2t_s^2)\tilde{\Lambda}_k^{-2} + (3 - 5t_s^2) \right] \quad (53)$$

where  $\sigma_1^{(B^2)} = \frac{e^4 \tau B^2 v_F^3}{8\pi^2 \hbar (1 - i\omega\tau) 15\mu^2}$ .

Obviously, from Eqs.(46) and (51),  $\sigma_{xx}^{(B^2, \Omega)}(\omega)$  and

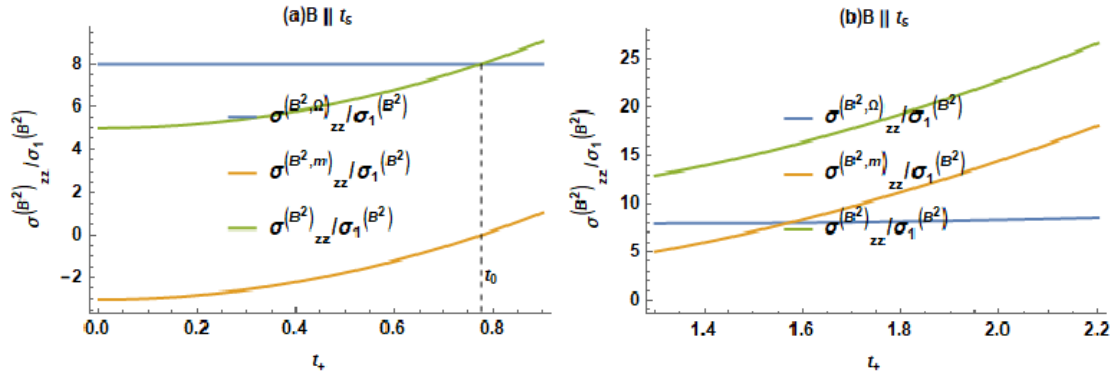


FIG. 6. The dependence of the optical conductivity on the tilt  $t_+$  for the case of  $B \parallel t_s$ . for (a) type-I WSM and (b) type-II WSM . The other parameters are the same as those of Fig.(1)

$\sigma_{xx}^{(B^2,m)}(\omega)$ , thus the total conductivity  $\sigma_{xx}^{(B^2)}(\omega)$  is equal to zero in the case of type-I WSM [50]. However, there is no such cancellation occur for type-II case. as shown in Fig.(5). Furthermore, in the case of type-I WSM, the total conductivity component  $\sigma_{zz}^{(B^2)}(\omega)$  is sup-

pressed(enforced) below(above) the value of  $t_0$  as shown in Fig.(6a)(see ref.[50]). For type-II WSM, the conductivity component  $\sigma_{zz}^{(B^2)}(\omega)$  the total conductivity is enhanced with tilt parameter  $t_0$  as shown in Fig.(6b).

Case-II In this case both longitudinal components as well as planer Hall conductivities are non-zero. The longitudinal components have the following expressions

for Type-I

$$\sigma_{xx}^{(B^2,\Omega)}(\omega) = \sigma_1^{(B^2)} \left[ (8 + 13t_s^2) \cos^2 \theta + \sin^2 \theta \right] \quad (54)$$

$$\sigma_{zz}^{(B^2,\Omega)}(\omega) = \sigma_1^{(B^2)} (1 + 7t_s^2) \quad (55)$$

for Type-II

$$\begin{aligned} \sigma_{xx}^{(B^2,\Omega)}(\omega) &= \frac{\sigma_1^{(B^2)}}{16t_s^5} \left[ \left\{ -55\tilde{\Lambda}_k^{-6} + 48(-4 + t_s^2)\tilde{\Lambda}_k^{-5} - 15(33 - 27t_s^2 + 4t_s^4)\tilde{\Lambda}_k^{-5} - 80(4 - 5t_s^2 + t_s^4)\tilde{\Lambda}_k^{-4} - 165(-1 + t_s^2)^2\tilde{\Lambda}_k^{-2} \right. \right. \\ &+ (1 + t_s^2) \left\{ 11 - 50t_s^2 + t_s^4(115 + 4t_s(8 + 15t_s)) \right\} \Lambda_s \left. \right\} \cos^2 \theta + \left\{ -5\tilde{\Lambda}_k^{-6} + 15(-3 + t_s^2)\tilde{\Lambda}_k^{-4} - 15(-1 + t_s^2)^2\tilde{\Lambda}_k^{-2} \right. \\ &+ \left. \left. \left\{ 1 + 5t_s^2(-1 + 3t_s^2 + t_s^4) \right\} \right\} \sin^2 \theta \right] \end{aligned} \quad (56)$$

$$\sigma_{zz}^{(B^2,\Omega)}(\omega) = \frac{\sigma_1^{(B^2)}}{4t_s^5} \left[ 10\tilde{\Lambda}_k^{-6} + 15(6 - 7t_s^2 + t_s^4)\tilde{\Lambda}_k^{-4} - 30k_F(-1 - t_s^2)^3\tilde{\Lambda}_k^{-2} \left\{ -2 + 11t_s^2 - 25t_s^4 + 65t_s^6 + 15t_s^8 \right\} \right] \quad (57)$$

The off-diagonal components of conductivities

for Type-I

$$\sigma_{xy}^{(B^2,\Omega)}(\omega) = \sigma_1^{(B^2)} (7 + 13t_s^2) \sin \theta \cos \theta \quad (58)$$

for Type-II

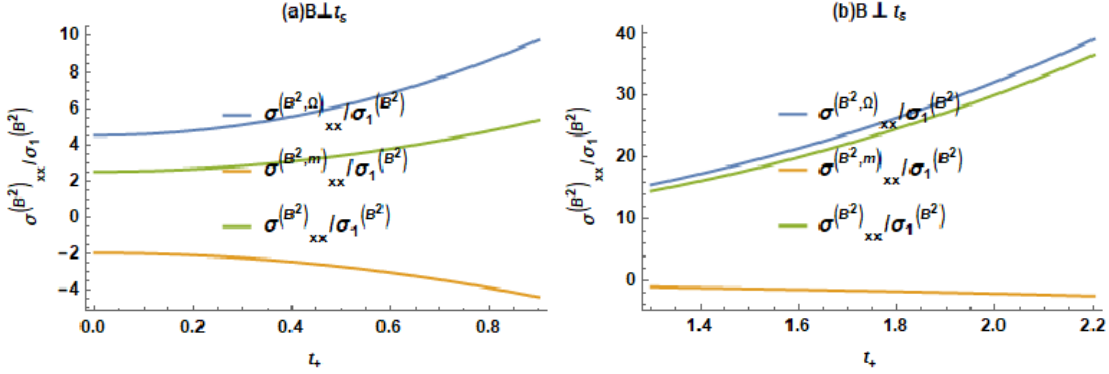


FIG. 7. The dependence of the optical conductivity on the tilt  $t_+$  for the case of  $B \perp t_s$ . for (a) type-I WSM and (b) type-II WSM at  $\theta = \frac{\pi}{4}$ . The other parameters are the same as those of Fig.(8)

$$\begin{aligned} \sigma_{xy}^{(B^2, \Omega)}(\omega) = & \frac{\sigma_1^{(B^2)}}{8t_s^5 \Lambda_s^6} \left[ -25\tilde{\Lambda}_k^{-6} + 24(-4 + t_s^2)\tilde{\Lambda}_k^{-5} - 15(-5 + t_s^2)(-3 + 2t_s^2)\tilde{\Lambda}_k^{-4} - 40(4 - 5t_s^2 + t_s^4)\tilde{\Lambda}_k^{-3} - 75k_F^2(-1 + t_s^2)^2\tilde{\Lambda}_k^{-2} \right. \\ & \left. + \left\{ 5 - 17t_s^2 + t_s^4 \{ 25 + t_s(16 + t_s(85 + 2t_s(8 + 15t_s))) \} \right\} \right] \sin \theta \cos \theta \end{aligned} \quad (59)$$

The magnetic orbital moment contributions of conductivities for Type-II  
for Type-I

$$\sigma_{xx}^{(B^2, m)}(\omega) = \sigma_1^{(B^2)} \left[ (-3 - 6t_s^2) \cos^2 \theta - \sin^2 \theta \right] \quad (60)$$

$$\sigma_{zz}^{(B^2, m)}(\omega) = \sigma_1^{(B^2)} (-1 + t_s^2) \quad (61)$$

$$\sigma_{xy}^{(B^2, m)}(\omega) = \sigma_1^{(B^2)} (-2 - 6t_s^2) \sin \theta \cos \theta \quad (62)$$

$$\begin{aligned} \sigma_{xx}^{(B^2, m)}(\omega) = & \frac{\sigma_1^{(B^2)}}{8t_s^5} \left[ \left\{ 85\tilde{\Lambda}_k^{-6} + 12(16 - 3t_s^2)\tilde{\Lambda}_k^{-5} + 45(17 - 3t_s^2)\tilde{\Lambda}_k^{-4} + 20k_F^3(16 - 17t_s^2 + 3t_s^4)\tilde{\Lambda}_k^{-3} + 15(17 - 18t_s^2 + t_s^4)\tilde{\Lambda}_k^{-2} \right. \right. \\ & - \left\{ 17 - 45t_s^2 + t_s^4(15 + t_s(32 + t_s(-35 + 24t_s))) \right\} \cos^2 \theta + \left\{ 15\tilde{\Lambda}_k^{-6} + 15(9 - 2t_s^2)\tilde{\Lambda}_k^{-4} + 15(3 - 4t_s^2 + t_s^4)\tilde{\Lambda}_k^{-2} \right. \\ & \left. \left. + (-3 + 10t_s^2 - 15t_s^4) \right\} \sin^2 \theta \right] \end{aligned} \quad (63)$$

$$\begin{aligned} \sigma_{zz}^{(B^2, m)}(\omega) = & \frac{-\sigma_1^{(B^2)}}{4t_s^5 \Lambda_s^6} \left[ 40\tilde{\Lambda}_k^{-6} - 6(-8 + t_s^2)\tilde{\Lambda}_k^{-5} + 15(24 - 5t_s^2)\tilde{\Lambda}_k^{-4} + 10(8 - 9t_s^2 + t_s^4)\tilde{\Lambda}_k^{-3} + 30(4 - 5t_s^2 + t_s^4)\tilde{\Lambda}_k^{-2} \right. \\ & + \left\{ -8 + 25t_s^2 - 30t_s^4 + 12t_s^5 + 5t_s^6 - 4t_s^7 \right\} \end{aligned} \quad (64)$$

$$\begin{aligned} \sigma_{xy}^{(B^2, m)}(\omega) = & \frac{\sigma_1^{(B^2)}}{8t_s^5} \left[ 50\tilde{\Lambda}_k^{-6} - 12(-8 + t_s^2)\tilde{\Lambda}_k^{-5} - 75(-6 + t_s^2)\tilde{\Lambda}_k^{-4} + 20(8 - 11t_s^2 + 3t_s^4)\tilde{\Lambda}_k^{-3} - 150 - 1 + t_s^2)\tilde{\Lambda}_k^{-2} \right. \\ & + \left\{ -10 + 25t_s^2 - 56t_s^5 + 25t_s^6 - 48t_s^7 \right\} \sin \theta \cos \theta \end{aligned} \quad (65)$$

It is noted that all the other magnetoconductivity

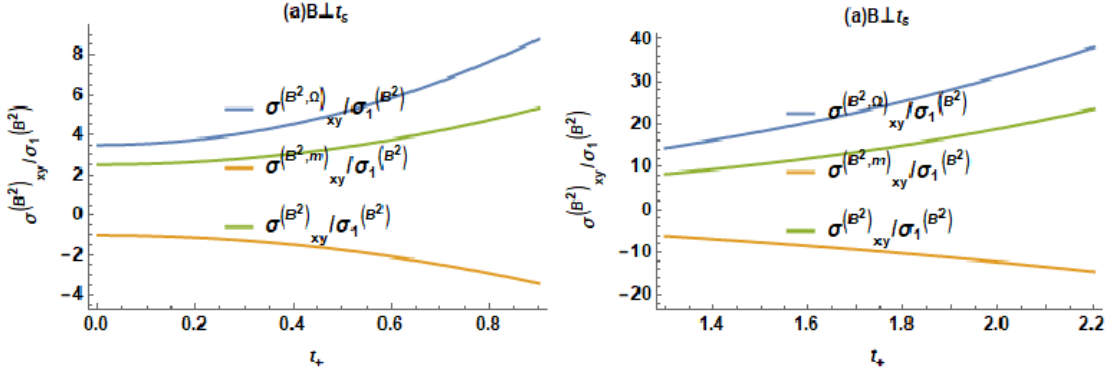


FIG. 9. The dependence of the planar Hall conductivity on the tilt  $t_+$  for the case of  $B \perp t_s$ , for (a) type-I WSM and (b) type-II WSM at  $\theta = \frac{\pi}{4}$ . The other parameters are the same as those of Fig.(1)

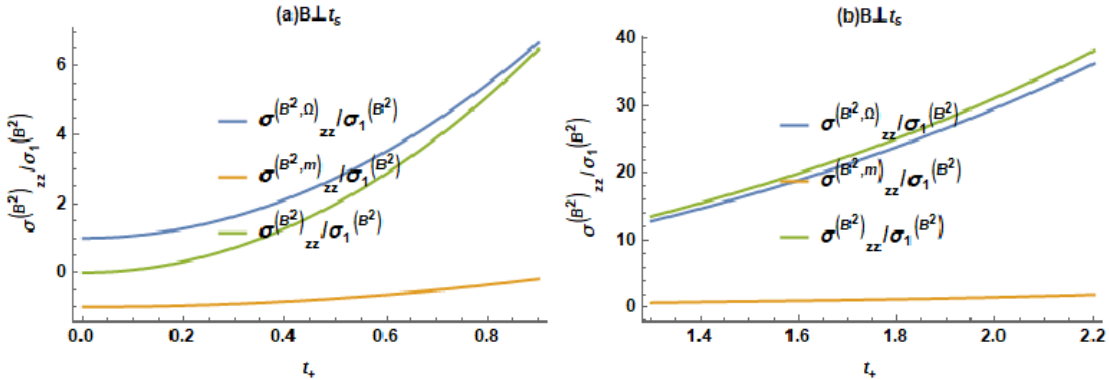


FIG. 8. The dependence of the optical conductivity on the tilt  $t_+$  for the case of  $B \perp t_s$ , for (a) type-I WSM and (b) type-II WSM. The other parameters are the same as those of Fig.(1)

components are zero. It is clear that the above conductivity equations are independent of chirality, i.e., the Weyl cones with opposite chiralities have the same contribution to the conductivity. The conductivity component  $\sigma_{xx}^{(B^2,m)}(\omega)$  for type-I and type-II are always negative, a result that will suppress the total conductivity compare to its Berry curvature parts.[see Fig(7)].

In the present system, the planar Hall effect can take place [51, 59–63] and manifest itself in a nonzero conductivity  $\sigma_{xy}^{(B^2)}(\omega)$ . Similar to the diagonal component of the conductivity,  $\sigma_{xy}^{(B^2)}(\omega)$  also consists of the contributions from the Berry curvature and the orbital magnetic moment. Figure (9) shows an effect of the tilt on the planar Hall magnetoconductivity. It is seen that the total planar Hall conductivity is suppressed in

Further, the conductivity component  $\sigma_{zz}^{(B^2,m)}(\omega)$  for type-I/II is always negative/positive, a result that will suppress/enhance the total conductivity compare to its Berry curvature parts.[see Fig(8)].

the case of type-I and type-II WSMs when the orbit magnetic moment is present as shown in Fig.(??). Figure (??) shows the planar Hall magnetoconductivity as a function of the THz incident light at  $\gamma = \pi/4$ . The real and imaginary parts of total conductivities are suppressed due to negative contribution of real and imaginary parts of magnetic orbital moment conductivities.

The  $B^2$  dependence of the magnetoconductivity has

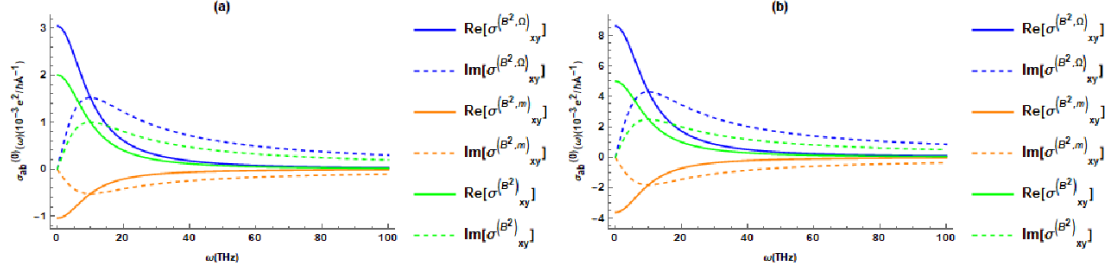


FIG. 10. The frequency dependence of optical conductivity on the tilt for the case of  $B \perp t_s$ . for (a) type-I WSM at  $t_+ = 0.5$  and (b) type-II WSM at  $t_+ = 1.3$ ,  $\theta = \frac{\pi}{4}$  and  $B = 1$  T. The other parameters are the same as those of Fig.(1)

been observed experimentally in the materials such as GdPtBi and TaP [62, 63]. TaS and GdPtBi have isotropic and quadratic band dispersions respectively. Therefore they are examples of single and double WSMs respectively. Recently, it is also shown that in the

materials GdPtBi, a very strong planar Hall effect has been reported, which is due to the Berry curvature and chiral anomaly contributions [62]. Besides chiral anomaly, the planar Hall effect may be induced by the orbital magnetic moment.

#### D. Hall conductivities $\sigma_{ab}^{(H,0)}$ and $\sigma_{ab}^{(H,B)}$

The intrinsic Hall effect is engendered by the Berry curvature, as presented by the second term of Eq. (17), for which further calculation gives

$$\sigma_{ab}^{(H)} = \sigma_{ab}^{(H,0)} + \sigma_{ab}^{(H,B)} \quad (66)$$

where

$$\sigma_{ab}^{(H,0)}(\omega) = -\frac{e^2}{\hbar(2\pi)^3} \epsilon_{abc} \int d^3k \Omega_c^s f_0^s \quad (67)$$

$$\sigma_{ab}^{(H,0)}(\omega) = \frac{e^2}{\hbar(2\pi)^3} \epsilon_{abc} \int d^3k \Omega_c^s (\mathbf{m}_k^s \cdot \mathbf{B}) \left( \frac{\partial f_0^s}{\partial \epsilon_k^s} \right) \quad (68)$$

where  $\epsilon_{abc}$  is the Levi-Civita symbol with  $a, b, c \in x, y, z$ . The first term  $\sigma_{ab}^{(H,0)}(\omega)$  in Eq. (66), referring to the anomalous Hall effect, is not equivalent to zero only in the system with broken time-reversal symmetry [36, 50]. While the second term  $\sigma_{ab}^{(H,0)}(\omega)$  stands for the ordinary Hall conductivity linear in  $B$ , which is the counterpart to a semiclassical description related to Landau level

formation in the quantum limit [49].

Let the magnetic field in spherical polar co-ordinate system  $\mathbf{B} = (B_x, B_y, B_z)$  with  $B_x = B \sin \theta \cos \phi$ ,  $B_y = B \sin \theta \sin \phi$ ,  $B_z = B \cos \theta$ . For a single Weyl node, the B-linear contribution to the Hall conductivity can be written as

$$\sigma_{ab}^{(H,B)} = \begin{pmatrix} 0 & \sigma_1^H \cos \theta & -\sigma_1^H \sin \theta \sin \phi \\ -\sigma_1^H \cos \theta & 0 & \sigma_1^H \sin \theta \cos \phi \\ \sigma_1^H \sin \theta \sin \phi & -\sigma_1^H \sin \theta \cos \phi & 0 \end{pmatrix} \quad (69)$$

where  
for Type-I

$$\sigma_1^H = -\frac{e^3}{\hbar} \frac{B v_F}{24\pi^2 \mu} \quad (70)$$

for Type-II

$$\sigma_1^H = -\frac{e^3}{\hbar} \frac{B v_F (\tilde{\Lambda}_k^{-3} + 3\tilde{\Lambda}_k^{-1} - t_s^3)}{24\pi^2 \mu t_s^3} \quad (71)$$

#### IV. SECOND ORDER NON-LINEAR RESPONSE OF TILTED-WSMS

In contrast to the type-I WSM node, the B-linear contribution to the Hall conductivity of type-II WSMs depends on the tilt parameter  $t_s$  as shown in Fig.(11).

Now, we explore the second-order nonlinear magneto-optical response of Weyl semimetals. Substituting Eq.(9) into Eq.(10), neglecting the Lorentz force term, and re-

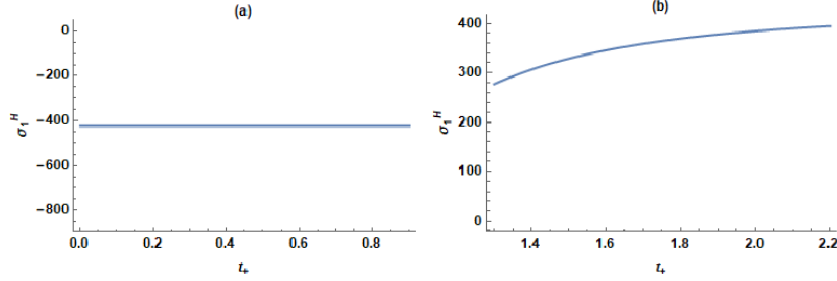


FIG. 11. The dependence of Hall conductivity on the tilt  $t_+$  for (a) type-I WSM and (b) type-II WSM. The other parameters are the same as those of Fig.(1)

taining terms up to second order in  $\mathbf{E}$ , we obtain

$$\frac{1}{\hbar D} \left[ -e\mathbf{E} - \frac{e^2}{\hbar} (\mathbf{E} \cdot \mathbf{B}) \Omega_{\mathbf{k}}^s \right] \cdot \frac{\partial \tilde{f}_1^s}{\partial \mathbf{k}} - i\omega \tilde{f}_2^s = -\frac{\tilde{f}_2^s}{\tau} \quad (72)$$

]

Solve for  $\tilde{f}_2^s$ , we obtain

$$\tilde{f}_2^s = \frac{\tau}{(1 - 2i\omega\tau)} \frac{1}{\hbar D} \left[ e\mathbf{E} + \frac{e^2}{\hbar} (\mathbf{E} \cdot \mathbf{B}) \Omega_{\mathbf{k}}^s \right] \cdot \frac{\partial \tilde{f}_1^s}{\partial \mathbf{k}} \quad (73)$$

Substituting Eq.(15) into Eq.(73) and retain terms up to first order in  $\mathbf{B}$ , we obtain

$$\begin{aligned} \tilde{f}_2^s = & \frac{e\tau^2}{\hbar(1 - i\omega\tau)(1 - 2i\omega\tau)} \left\{ \mathbf{E} \cdot \frac{\partial}{\partial \mathbf{k}} \left[ \left( e\mathbf{E} + \frac{e^2}{\hbar} (\mathbf{E} \cdot \mathbf{B}) \Omega_{\mathbf{k}}^s - \frac{e^2}{\hbar} (\mathbf{B} \cdot \Omega_{\mathbf{k}}^s) \mathbf{E} \right) \cdot \mathbf{v}_{\mathbf{k}}^s \frac{\partial f_0^s}{\partial \epsilon_{\mathbf{k}}^s} - \frac{e}{\hbar} \mathbf{E} \cdot \frac{\partial}{\partial \mathbf{k}} \left( \mathbf{m}_{\mathbf{k}}^s \cdot \mathbf{B} \frac{\partial f_0^s}{\partial \epsilon_{\mathbf{k}}^s} \right) \right] \right. \\ & \left. + \left[ \frac{e^2}{\hbar} (\mathbf{E} \cdot \mathbf{B}) \Omega_{\mathbf{k}}^s - \frac{e^2}{\hbar} (\mathbf{B} \cdot \Omega_{\mathbf{k}}^s) \mathbf{E} \right] \cdot \frac{\partial}{\partial \mathbf{k}} \left( \mathbf{E} \cdot \mathbf{v}_{\mathbf{k}}^s \frac{\partial f_0^s}{\partial \epsilon_{\mathbf{k}}^s} \right) \right\} \end{aligned} \quad (74)$$

Now the electric current density at the frequency  $2\omega$  is given by

$$\begin{aligned} \mathbf{j}_1 = & -\frac{e}{(2\pi)^3} \int d^3k \left[ \tilde{\mathbf{v}}_{\mathbf{k}}^s + \frac{e}{\hbar} (\Omega_{\mathbf{k}}^s \cdot \tilde{\mathbf{v}}_{\mathbf{k}}^s) \mathbf{B} \right] \tilde{f}_2^s \\ = & \frac{e^2}{2\pi)^3 \hbar} \int d^3k \mathbf{E} \times \Omega_{\mathbf{k}}^s \tilde{f}_1^s \end{aligned} \quad (75)$$

According to the definition of second harmonic conductivity, this equation should be written in the form

$$\mathbf{j}(2\omega) = \sigma(2\omega) \mathbf{E}(\omega) \mathbf{E}(\omega) \quad (76)$$

where  $\sigma(2\omega)$  is the second harmonic conductivity.

### A. Second harmonic conductivity $\sigma_{abc}^0$ in the absence of magnetic field

In this subsection, we calculate the second harmonic current of the Weyl semimetals system in the absence

of magnetic fields  $\mathbf{B} = 0$ . Inserting Eq. (74) into the first term of Eq. (75), the second harmonic conductivity tensor can be written as

$$\sigma_{abc}^0(2\omega) = \frac{-\tau^2}{(1 - i\omega\tau)(1 - 2i\omega\tau)} \frac{e^3}{\hbar(2\pi)^3} \int d^3k \frac{\partial v_a^s}{\partial k_c} v_b^s \left( -\frac{\partial f_0^s}{\partial \epsilon_{\mathbf{k}}^s} \right) \quad (77)$$

Except for the aaz, aza, and zaa ( $a = x, y, z$ ) components of the second harmonic conductivity tensor are nonzero and all other components equal to zero [50, 64]

for Type-I

$$\sigma_{zzz}^0(2\omega) = 2\sigma_{DL} \left[ \frac{-6 + 4t_s^2}{t_s^3} - \frac{3(1 - t_s^2)}{t_s^4} \ln \frac{1 - t_s}{1 + t_s} \right] \quad (78)$$

$$\sigma_{xxz}^0(2\omega) = \sigma_{DL} \left[ \frac{6}{t_s^3} + \frac{3 - t_s^2}{t_s^4} \ln \frac{1 - t_s}{1 + t_s} \right] \quad (79)$$

for Type-II

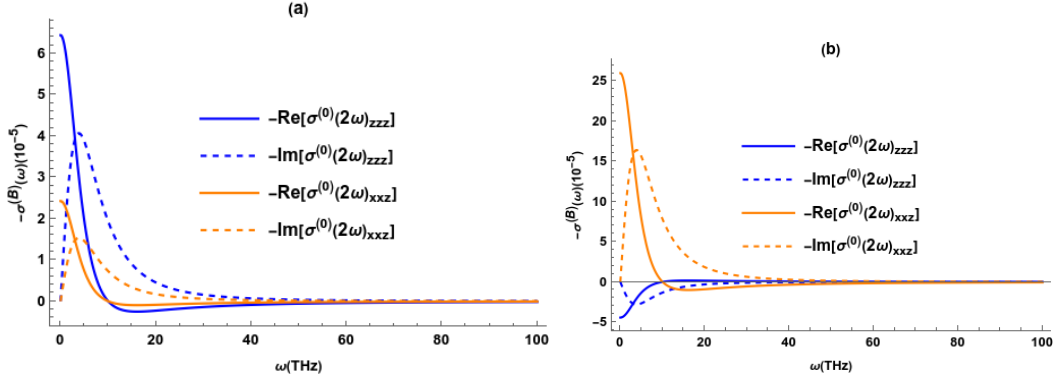


FIG. 13. The frequency dependence of optical conductivity on tilt for the process of second harmonic generation. for (a) type-I WSM at  $t_+ = 0.5$  and (b) type-II WSM at  $t_+ = 1.3$ . The other parameters are the same as those of Fig.(1)

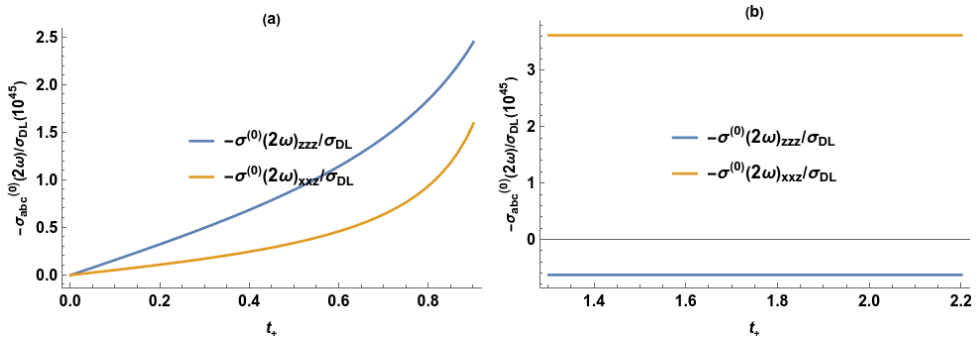


FIG. 12. The dependence of the nonlinear optical conductivities for the process of second harmonic generation of on tilt  $t_+$ , for (a) type-I WSM and (b) type-II WSM .The other parameters are the same as those of Fig.(1)

$$\sigma_{zzz}^0(2\omega) = -\frac{2\sigma_{DL}}{t_s^4} \left[ -\tilde{\Lambda}_k^{-2} + (-3 + t_s^2) - 3(-1 + t_s^2) \ln[(t_s^2 - 1)\tilde{\Lambda}_k^2] \right] \quad (80)$$

$$\sigma_{xxz}^0(2\omega) = \frac{\tilde{\Lambda}_k \sigma_{DL}}{t_s^4} \left[ 2\tilde{\Lambda}_k^{-2}(-3 + t_s^2) + 6t_s\tilde{\Lambda}_k^{-1} - 2(-1 + t_s^4) - (-3 + t_s^2)\tilde{\Lambda}_k^{-1} \ln \frac{t_s - 1}{t_s + 1} \right] \quad (81)$$

where  $\sigma_{DL} = \frac{e^3 \tau^2 \mu}{(1-2i\omega\tau)(1-i\omega\tau)8\pi^2\hbar^3}$  is the Drude-like

frequency dependent complex conductivity.

The second harmonic conductivity tensor satisfies the relation  $\sigma_{zxx}^0(2\omega) = \sigma_{zyy}^0(2\omega) = \sigma_{xzx}^0(2\omega) = \sigma_{yzy}^0(2\omega) = \sigma_{xxz}^0(2\omega) = \sigma_{yyz}^0(2\omega)$ , and it does not depend on the chirality of Weyl node. The total second harmonic conductivity in tilted Weyl semimetals is the sum of a pair of Weyl nodes. For the case with tilt inversion symmetry  $t_+ = -t_-$ ,  $\sigma_{abc}(2\omega) = 0$ . For the case with

broken tilt inversion symmetry  $t_+ = t_-$ ,  $\sigma_{abc}(2\omega) \neq 0$ .

It is noted to see from Fig.(12a) that the  $\sigma_{abc}^0(2\omega)$  becomes exactly zero when  $t_s \rightarrow 0$  and the presence of the finite tilt is needed to get the second harmonic generation in type-I WSMs. It is also evident from Fig.(12a) that  $\sigma_{zzz}^0(2\omega)$  is more sensitive to tilt than  $\sigma_{xxz}^0(2\omega)$  in type-I WSMs [50]. Fig.(12b) shows that  $\sigma_{zzz}^0(2\omega)$  has opposite behavior with tilt parameter as compare to  $\sigma_{xxz}^0(2\omega)$ . Fig.(13) shows the frequency variation of tilted-WSMs.

## B. Second harmonic conductivity $\sigma_{abc}^B$ in the presence of linear magnetic field

Inserting Eq. (74) into the first term of Eq. (75), we write the linear  $\mathbf{B}$  dependent second harmonic conduc-

tivity tensor

---


$$\begin{aligned} \sigma_{abc}^B(2\omega) = & \frac{\tau^2}{(1-i\omega\tau)(1-2i\omega\tau)} \frac{e^3}{\hbar(2\pi)^3} \int d^3k \left\{ \frac{\partial v_a^s}{\partial k_c} \left[ -\frac{eB_b}{\hbar} (\Omega_k^s \cdot \mathbf{v}_k^s) + \frac{ev_b^s}{\hbar} (\Omega_k^s \cdot \mathbf{B}) \right] - \frac{eB_c}{\hbar} \frac{\partial}{\partial \mathbf{k}} \cdot (v_a^s \Omega_k^s) v_b^s \right. \\ & \left. + \frac{e}{\hbar} \frac{\partial [v_a^s (\Omega_k^s \cdot \mathbf{B})]}{\partial k_c} v_b^s - \frac{eB_a}{\hbar} \frac{\partial (\Omega_k^s \cdot \mathbf{v}_k^s)}{\partial k_c} v_b^s + \frac{\partial^2 (\mathbf{m}_k^s \cdot \mathbf{B})}{\hbar \partial k_a \partial k_c} v_b^s - \frac{\partial^2 v_a^s}{\hbar \partial k_a \partial k_c} (\mathbf{m}_k^s \cdot \mathbf{B}) \right\} \left( -\frac{\partial f_0^s}{\partial \epsilon_k^s} \right) \end{aligned} \quad (82)$$

We will explore Eq.(82) with following two cases:

for type-I

$$\sigma_{xzx}^B(2\omega) = s \frac{2}{3} \sigma_2^{(B)} \quad (83)$$

$$\sigma_{zxx}^B(2\omega) = -s \frac{2}{3} \sigma_2^{(B)} \quad (84)$$

Case-I In the case of  $\mathbf{B} \parallel t_s$ , for a single Weyl node, we obtain the magnetoconductivity components

for type-II

$$\begin{aligned} \sigma_{xzx}^B(2\omega) = & s \frac{\sigma_2^{(B)}}{60t_s^3} \left[ -60\tilde{\Lambda}_k^{-4} + 40\tilde{\Lambda}_k^{-3} + 60(-5 + t_s^2)\tilde{\Lambda}_k^{-2} + 15(8 - 5t_s^2)\tilde{\Lambda}_k^{-1} + \left\{ -40 + t_s^2(45 + 32t_s) \right\} \right. \\ & \left. + 3t_s^3 \sin \left[ 5 \csc^{-1} \left( \frac{t_s \Lambda_k}{k_F + \Lambda_k} \right) \right] \right] \end{aligned} \quad (85)$$

$$\begin{aligned} \sigma_{zxx}^B(2\omega) = & -s \frac{\sigma_2^{(B)}}{60t_s^3} \left[ 120\tilde{\Lambda}_k^{-2} + 30t_s^2\tilde{\Lambda}_k^{-1} - 2 \left\{ -20 + t_s^2 + t_s^2(45 + 14t_s) \right\} + t_s^3 \left\{ 5 \sin \left[ 3 \csc^{-1} \left( \frac{t_s \Lambda_k}{k_F + \Lambda_k} \right) \right] \right. \right. \\ & \left. \left. + 3 \sin \left[ 5 \csc^{-1} \left( \frac{t_s \Lambda_k}{k_F + \Lambda_k} \right) \right] \right\} \right] \end{aligned} \quad (86)$$

where  $\sigma_2^{(B)} = \frac{e^4 \tau^2 B v_F^2}{\hbar^2 (1-2i\omega\tau)(1-i\omega\tau) 8\pi^2 \mu}$

We can check that other nonzero second harmonic conductivity components satisfy the relations:  $\sigma_{zxx}^B(2\omega) = \sigma_{zyy}^B(2\omega) = \sigma_{xzx}^B(2\omega) = \sigma_{yzy}^B(2\omega)$ . In contrast to type-I WSMs, the B-linear contribution to the second harmonic conductivity depends on the tilt in type-II WSMs. Summing the conductivity over the Weyl cones with opposite chirality cancels each other, leading to the disappearance of the total B-linear contribution to the second harmonic conductivity.

Case-II In the case of  $\mathbf{B} \perp t_s$ , we get the nonzero

conductivity components

for type-I

$$\sigma_{zxx}^{(B)}(2\omega) = s \frac{2}{3} \sigma_2^{(B)} \cos \theta \quad (87)$$

$$\sigma_{xzx}^{(B)}(2\omega) = -s \frac{2}{3} \sigma_2^{(B)} \cos \theta \quad (88)$$

$$\sigma_{zyz}^{(B)}(2\omega) = s \frac{2}{3} \sigma_2^{(B)} \sin \theta \quad (89)$$

$$\sigma_{yzz}^{(B)}(2\omega) = -s \frac{2}{3} \sigma_2^{(B)} \sin \theta \quad (90)$$

for type-II

$$\begin{aligned}\sigma_{zxz}^{(B)}(2\omega) &= s \frac{\sigma_2^{(B)}}{120t_s^3} \left[ 90\tilde{\Lambda}_k^{-4} - 220\tilde{\Lambda}_k^{-3} + 60(8 - 3t_s^2)\tilde{\Lambda}_k^{-2} + 45(-4 + 3t_s^2)\tilde{\Lambda}_k^{-1} + \left\{ 70 + t_s^2(-165 + 64t_s + 90t_s^2) \right\} \right. \\ &\quad \left. + 3t_s^3 \left\{ 10 \cos \left[ \sec^{-1} \left( \frac{t_s}{1 + \tilde{\Lambda}_k^{-1}} \right) \right] - 3 \sin \left[ 5 \csc^{-1} \left( \frac{t_s}{1 + \tilde{\Lambda}_k^{-1}} \right) \right] \cos \theta \right\} \right] \quad (91)\end{aligned}$$

$$\begin{aligned}\sigma_{xzz}^{(B)}(2\omega) &= s \frac{\sigma_2^{(B)}}{60t_s^5} \left[ 36\tilde{\Lambda}_k^{-5} + 15(12 - 11t_s^2)\tilde{\Lambda}_k^{-4} + 40(9 - 23t_s^2 + 3t_s^4)\tilde{\Lambda}_k^{-3} + 30(12 - 39t_s^2 + 7t_s^4)\tilde{\Lambda}_k^{-2} \right. \\ &\quad \left. - 60(-3 + 18t_s^2 - 13t_s^4 + 2t_s^6)\tilde{\Lambda}_k^{-1} + \left\{ 36 - t_s^2 \{ 225 + t_s^2(-210 + t_s(16 + 45t_s)) \} \right\} \right] \cos \theta \quad (92)\end{aligned}$$

$$\begin{aligned}\sigma_{zyz}^{(B)}(2\omega) &= s \frac{\sigma_2^{(B)}}{120t_s^3} \left[ 90\tilde{\Lambda}_k^{-4} - 220\tilde{\Lambda}_k^{-3} + 60(8 - 3t_s^2)\tilde{\Lambda}_k^{-2} + 45(-4 + 3t_s^2)\tilde{\Lambda}_k^{-1} + \left\{ 70 + t_s^2(-165 + 64t_s + 90t_s^2) \right\} \right. \\ &\quad \left. + 3t_s^3 \left\{ 10 \cos \left[ \sec^{-1} \left( \frac{t_s}{1 + \tilde{\Lambda}_k^{-1}} \right) \right] - 3 \sin \left[ 5 \csc^{-1} \left( \frac{t_s}{1 + \tilde{\Lambda}_k^{-1}} \right) \right] \sin \theta \right\} \right] \quad (93)\end{aligned}$$

$$\begin{aligned}\sigma_{yzz}^{(B)}(2\omega) &= s \frac{\sigma_2^{(B)}}{60t_s^5} \left[ 132\tilde{\Lambda}_k^{-5} - 165(-4 + t_s^2)\tilde{\Lambda}_k^{-4} + 40(33 - 25t_s^2 + 3t_s^4)\tilde{\Lambda}_k^{-3} + 30(44 - 47t_s^2 + 7t_s^4)\tilde{\Lambda}_k^{-2} \right. \\ &\quad \left. - 15(-44 + 88t_s^2 - 45t_s^4 + 8t_s^6)\tilde{\Lambda}_k^{-1} + (132 - 305t_s^2 + 105t_s^4 + 73t_s^5 - 45t_s^6) \right] \sin \theta \quad (94)\end{aligned}$$

In this case, the B-linear contribution to the second harmonic conductivity is dependent on the chirality but independent(dependent) of the tilt in type-I(type-II) WSMs. Summing the conductivity over the Weyl cones with opposite chirality cancels each other, leading to the disappearance of the total B-linear contribution to the second harmonic conductivity.

$$\sigma_{abc}^{(H,0)} = \epsilon_{acd} \frac{e^3 \tau}{\hbar^2 (1 - i\omega\tau)} D_{bd} \quad (95)$$

where  $D_{bd}$  is called Berry dipole. It is a first-order moment of the Berry curvature[65].

One can calculate the non-zero components of Berry curvature dipole

$$D_{bd} = \frac{\hbar}{(2\pi)^3} \int d^3k \Omega_d^s v_b^s \left( -\frac{\partial f_0^s}{\partial \epsilon_k^s} \right) \quad (96)$$

for type-I

$$D_{xx} = D_{yy} = -s \frac{1}{16\pi^2} \left[ \frac{2}{t_s} + \frac{1 - t_s^2}{t_s^3} \ln \frac{1 - t_s}{1 + t_s} \right] \quad (97)$$

$$D_{zz} = -s \frac{1}{8\pi^2} \frac{t_s^2 - 1}{t_s^3} \left[ 2t_s + \ln \frac{1 - t_s}{1 + t_s} \right] \quad (98)$$

for type-II

$$D_{xx} = D_{yy} = s \frac{1}{16\pi^2 t_s^3} \left[ -\tilde{\Lambda}_k^{-2} + (-3 + t_s^2) + (-1 + t_s^2) \ln \left( \frac{1 + t_s}{t_s - 1} \right) \right] \quad (99)$$

$$D_{zz} = s \frac{1}{8\pi^2 t_s^3} \left[ 2(-1 + t_s^2)\tilde{\Lambda}_k^{-1} - 2t_s(-1 + t_s^2) + (-1 + t_s^2) \ln \left( \frac{1 + t_s}{t_s - 1} \right) \right] \quad (100)$$

In contrast to type-I WSMs, the magnitude of Berry curvature dipole components in type-II WSMs depends

on chemical potential to momentum cut off. They both depends on the chirality. of the Weyl nodes. Therefore,

contributions from a pair of Weyl nodes with opposite chirality exactly cancel each other [50, 64, 65].

#### D. Linear B-contribution to the second order nonlinear Hall conductivity $\sigma_{abc}^{(H,B)}$

Now, we focus on the second-order nonlinear Hall effect in a weak magnetic field. Inserting Eq. (16) into the second term of Eq. (75) and retaining terms up to the first power of B, one obtains complex nonlinear Hall conductivity

$$\sigma_{abc}^{(H,B)} = \epsilon_{acd} \frac{e^3 \tau}{\hbar^2 (1 - i\omega\tau)} [D_{bd}^\Omega + D_{bd}^m] \quad (101)$$

where

$$D_{bd}^\Omega = \frac{e}{(2\pi)^3} \int d^3k \Omega_d^s [B_b(\Omega_k^s \cdot \mathbf{v}_k^s) - v_b^s(\Omega_k^s \cdot \mathbf{B})] \left( -\frac{\partial f_0^s}{\partial \epsilon_k^s} \right) \quad (102)$$

$$D_{bd}^m = \frac{1}{(2\pi)^3} \int d^3k \frac{\partial \Omega_d^s}{\partial k_b} (\mathbf{m}_k^s \cdot \mathbf{B}) \left( -\frac{\partial f_0^s}{\partial \epsilon_k^s} \right) \quad (103)$$

where  $D_{bd}^\Omega$  and  $D_{bd}^m$  are Berry curvature dipole contributions due to the Berry curvature and the orbital magnetic moment, respectively.

Again we will consider the following two cases.

Case I In the case of  $\mathbf{B} \parallel t_s$ , one obtains the Berry curvature dipole components.

for type-I

$$D_{xx}^\Omega = D_{yy}^\Omega = -t_s D_2^{(B)} \quad (104)$$

$$D_{zz}^m = t_s D_2^{(B)} \quad (105)$$

$$D_{xx}^m = D_{yy}^m = 2t_s D_2^{(B)} \quad (106)$$

$$D_{zz}^m = -4t_s D_2^{(B)} \quad (107)$$

for type-II

$$D_{xx}^\Omega = D_{yy}^\Omega = -\frac{D_2^{(B)}}{2t_s^4} [3\tilde{\Lambda}_k^{-5} - 5(-3 + t_s^2)\tilde{\Lambda}_k^{-3} + 2t_s^5] \quad (108)$$

$$D_{zz}^\Omega = \frac{D_2^{(B)}}{t_s^4} [3\tilde{\Lambda}_k^{-5} - 5(-3 + t_s^2)\tilde{\Lambda}_k^{-3} + 2t_s^5] \quad (109)$$

$$D_{xx}^m = D_{yy}^m = \frac{D_2^{(B)}}{2t_s^4} [-9\tilde{\Lambda}_k^{-5} + 5(-9 + t_s^2)\tilde{\Lambda}_k^{-3} + 4t_s^5] \quad (110)$$

$$D_{zz}^m = \frac{D_2^{(B)}}{t_s^4} [9\tilde{\Lambda}_k^{-5} - 5(-9 + t_s^2)\tilde{\Lambda}_k^{-3} - 4t_s^5] \quad (111)$$

where,  $D_2^{(B)} = \frac{1}{8\pi^2} \frac{eB}{\hbar} \frac{\hbar^2 v_F^2}{15\mu^2}$ . In contrast to type-I WSMs, the magnitude of Berry curvature dipole components in type-II WSMs depends on chemical potential to momentum cut off.

Case-II In the case of  $\mathbf{B} \perp t_s$ , we get the nonzero components

for type-I

$$D_{zx}^\Omega = -6t_s D_2^{(B)} \cos \theta \quad (112)$$

$$D_{xz}^\Omega = 9t_s D_2^{(B)} \cos \theta \quad (113)$$

$$D_{zy}^\Omega = -6t_s D_2^{(B)} \sin \theta \quad (114)$$

$$D_{yz}^\Omega = 9t_s D_2^{(B)} \sin \theta \quad (115)$$

and

$$D_{zx}^m = -3t_s D_2^{(B)} \cos \theta \quad (116)$$

$$D_{zy}^m = -3t_s D_2^{(B)} \sin \theta \quad (117)$$

for type-II

$$D_{zx}^\Omega = -\frac{3D_2^{(B)}}{8t_s^4} \left[ 5(-3+t_s^2)\tilde{\Lambda}_k^{-4} - 10(-1+t_s^2)^2\tilde{\Lambda}_k^{-2} + \left\{ 1 + 5t_s^2(-1+3t_s^2+t_s^4) \right\} \right] \cos \theta \quad (118)$$

$$\begin{aligned} D_{xz}^\Omega &= \frac{D_2^{(B)}}{4t_s^4} \left[ 6\tilde{\Lambda}_k^{-5} - 15(-3+t_s^2)\tilde{\Lambda}_k^{-4} - 10(-3+t_s^2)\tilde{\Lambda}_k^{-3} - 30(-1+t_s^2)\tilde{\Lambda}_k^{-2} \right. \\ &\quad \left. + \left\{ -3 + 5t_s^2 + t_s^2(15+t_s(4+15)) \right\} \right] \cos \theta \end{aligned} \quad (119)$$

$$D_{zy}^\Omega = -\frac{3D_2^{(B)}}{8t_s^4} \left[ 5(-3+t_s^2)\tilde{\Lambda}_k^{-4} - 10(-1+t_s^2)^2\tilde{\Lambda}_k^{-2} + \left\{ 1 + 5t_s^2(-1+3t_s^2+t_s^4) \right\} \right] \sin \theta \quad (120)$$

$$\begin{aligned} D_{yz}^\Omega &= \frac{D_2^{(B)}}{4t_s^4} \left[ 6\tilde{\Lambda}_k^{-5} - 15(-3+t_s^2)\tilde{\Lambda}_k^{-4} - 10(-3+t_s^2)\tilde{\Lambda}_k^{-3} - 30(-1+t_s^2)\tilde{\Lambda}_k^{-2} \right. \\ &\quad \left. + \left\{ -3 + 5t_s^2 + t_s^4(15+t_s(4+15t_s)) \right\} \right] \sin \theta \end{aligned} \quad (121)$$

and

$$\begin{aligned} D_{zx}^m &= -\frac{3D_2^{(B)}}{2t_s^4} \left[ 3\tilde{\Lambda}_k^{-5} - 5(-3+t_s^2)\tilde{\Lambda}_k^{-3} + 2t_s^5 \right] \cos \theta \\ D_{zy}^m &= -\frac{3D_2^{(B)}}{2t_s^4} \left[ 3\tilde{\Lambda}_k^{-5} - 5(-3+t_s^2)\tilde{\Lambda}_k^{-3} + 2t_s^5 \right] \sin \theta \end{aligned} \quad (122)$$

One can check that  $D_{zx}^m = D_{xz}^m$  and  $D_{zy}^m = D_{yz}^m$  and rest of the components will vanish. In contrast to type-I WSMs, the magnitude of Berry curvature dipole components in type-II WSMs depends on chemical potential to momentum cut off

The nonlinear Hall effect can be modulated by the polarization of the incident light, as discussed in Ref.[50]. Using Eq. (101), the electric current is rewritten in the form of

$$\mathbf{j}(2\omega) = \frac{e^3 \tau}{\hbar^2(1-i\omega\tau)} (\hat{D} \cdot \mathbf{E}) \times \mathbf{E} \quad (123)$$

Assume that an electromagnetic wave propagates in

the x direction:

$$\mathbf{E}(\mathbf{r}, t) = |\mathbf{E}(\omega)| Re[|\psi\rangle e^{i(qx - \omega t)}] \quad (124)$$

where

$$|\psi\rangle = \begin{pmatrix} \psi_y \\ \psi_z \end{pmatrix} = \begin{pmatrix} \sin \theta e^{i\alpha_y} \\ \cos \theta e^{i\alpha_z} \end{pmatrix} \quad (125)$$

is the Jones vector in the y-z plane with phases  $\alpha_y, \alpha_z$ , and the amplitudes  $E_y = |\mathbf{E}| \sin \theta$  and  $E_z = |\mathbf{E}| \cos \theta$ . Inserting Eq. (124) into Eq. (123), we obtain the nonlinear Hall current

$$j_x(2\omega) = \frac{e^3 \tau}{\hbar^2(1-i\omega\tau)} \frac{D_{yy}^{(B)} - D_{zz}^{(B)}}{2} \sin 2\theta e^{(\alpha_y + \alpha_z)} |\mathbf{E}|^2 \quad (126)$$

Following the same procedure of Ref.([50]), Eq.(126) can be rewritten as  $j_x \sim (D_{yy} - D_{zz}) E_y E_z$ . Hence conductivity will be

for type-I

$$\sigma_x^{(H,B)}(2\omega) = \frac{e^3 \tau}{(1-i\omega\tau)\hbar^2} \frac{3t_s}{2} D_2^{(B)} \sin 2\theta \quad (127)$$

for type-II

$$\sigma_x^{(H,B)}(2\omega) = \frac{-e^3 \tau}{(1-i\omega\tau)\hbar^2} \frac{1}{4t_s^4} \left[ 72\tilde{\Lambda}_k^{-5} + 135\tilde{\Lambda}_k^{-4} - 60(-3+t_s^2)\tilde{\Lambda}_k^{-3} + (-9+10t_s^2+15t_s^4-12t_s^5) \right] D_2^{(B)} \sin 2\theta \quad (128)$$

Fig.(14) shows the variation of linear-B second har-

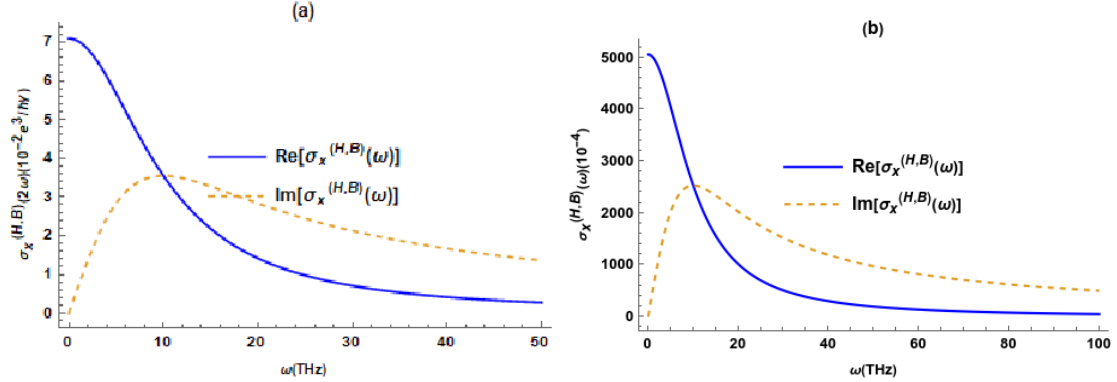


FIG. 14. The nonlinear Hall conductivities for the process of second harmonic generation as a function of the incident photon frequency on the tilt .for (a) type-I WSM at  $t_+ = 0.5$ (b) type-II WSM at  $t_+ = 1.3$  . The other parameters are the same as those of Fig.(1)

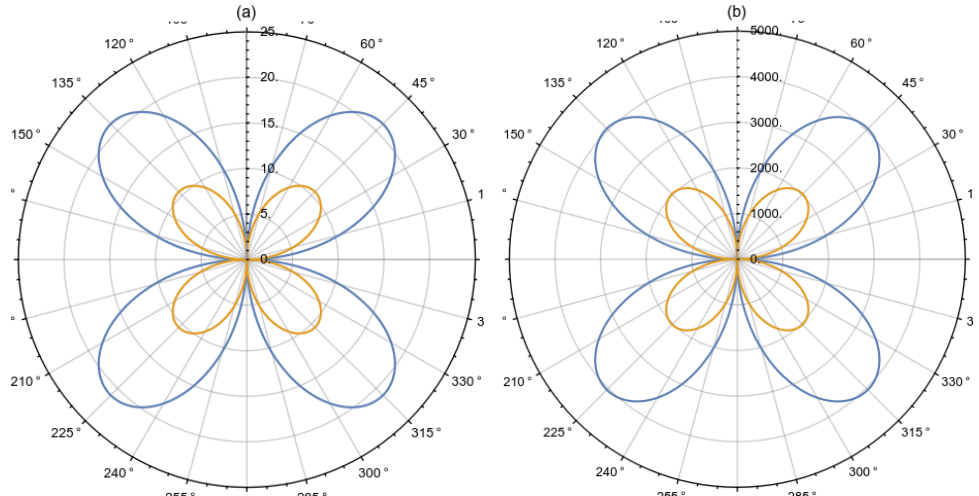


FIG. 15. The angle dependence of the nonlinear Hall conductivity at  $\omega = 5$  THz for (a) type-I WSM at  $t_+ = 0.5$ (b) type-II WSM at  $t_+ = 1.3$  . The other parameters are the same as those of Fig.(1)

monic conductivities  $\sigma_x^{(H,B)}(2\omega)$  as function of incident photon frequency  $\omega$ . In contrast to the case of  $B = 0$ , the B-linear contribution to the nonlinear Hall conductivity is independent of the chirality, and the odd function of  $t_s$  . Only in the system with broken tilt inversion symmetry ( $t_+ = t_-$  ), the conductivity  $\sigma_x^{(H,B)}(2\omega) \neq 0$ . From Eq.(127) and (128), evidently,  $\sigma_x^{(H,B)}(2\omega)$  reaches its maximum when the polarization direction  $\theta = \pm\pi/4$  and vanishes at  $\theta = 0, \pi/2$ , as further reflected in Fig(15).

Recent experiments shows the second harmonic optical response generates gaint second-order nonlinear optical polarizability,  $\chi^2$ , in transition metal monopnictides (TMMPs) such as TaAs, a class of noncentrosymmetric materials [66]. Another experiment reports large non-linear Hall effect(NLHE) due to gigantic Berry curvature dipole density as generated by tilted Weyl cones near the Fermi level in a model ferroelectric Weyl

semimetal in doped  $(Pb_{1-x}Sn_x)_{1-y}In_yTe$ . The effective Berry curvature dipole derived from the experimentally observed nonlinear Hall voltage follows a scaling law with carrier concentration, which is consistent with the simplest form of the Berry curvature dipole expected for the Weyl monopoles [67].

## V. CONCLUSION

We have calculated the magneto-optical conductivities of gapless type-I and type-II Weyl semimetals in the presence of orbital magnetic moment in linear and non-linear responses within the semiclassical Boltzmann approach and compared them. We have found that the total conductivity elements are suppressed due to OMM in most of the responses except quadratic

response of  $\sigma_z z(B^2)$  in type-II WSMs. The magnitudes of conductivity components due to both Berry curvature and OMM have large magnitudes in type-II WSMs due to finite density of states near Weyl points.

## Appendix A: DETAILS OF THE CALCULATIONS USING SPHERICAL POLAR COORDINATES

In this paper, we have focused on the n-doped tilted Weyl semimetals with a positive chemical potential  $\mu$ . In general, one can decompose the momentum  $\mathbf{k}$  using spherical co-ordinates as follow

$$k_x = k \sin \theta \cos \phi \quad (\text{A1})$$

$$k_y = k \sin \theta \sin \phi \quad (\text{A2})$$

$$k_z = k \cos \theta \quad (\text{A3})$$

The Jacobian of the transformation is  $\mathcal{J} = k^2 \sin \theta$ , which has been used for analytical expressions of conductivity elements of tilted-WSMs.

For type-II WSM, we introduce a finite cut-off  $\Lambda_k$  such that  $\Lambda_k(1 + t_s) > k_F$  in the radial direction  $\mathbf{k}$ . For the conduction band with  $t_s > 1$  we obtain the integration limit to be

$$\left( \frac{k_F}{\Lambda_k} - 1 \right) \frac{1}{t_s} \leq x \leq 1, \quad (\text{A4})$$

with  $\Lambda_k(t_s + 1) > k_F$ . The left hand side term of this inequality is negative for  $t_s > 0$ . When  $t_s < -1$ , we get

$$-1 \leq x \leq \left( \frac{k_F}{\Lambda_k} - 1 \right) \frac{1}{t_s}, \quad (\text{A5})$$

with  $\Lambda_k(-t_s + 1) > k_F$ . Similarly, we get the following limit for the valence band

$$\left( \frac{k_F}{\Lambda_k} + 1 \right) \frac{1}{t_s} \leq x \leq 1, \quad (\text{A6})$$

with  $\Lambda_k(t_s - 1) > k_F$  for  $t_s > 1$ . For  $t_s < -1$ , we get the following limit

$$-1 \leq x \leq \left( \frac{k_F}{\Lambda_k} + 1 \right) \frac{1}{t_s}, \quad (\text{A7})$$

with  $-\Lambda_k(t_s + 1) > k_F$ . For the calculation of conductivities, all these limits are essential for performing all the integrals.

---

[1] H. Weyl *et al.*, Electron and gravitation, *z. Phys* **56**, 330 (1929).

[2] S.-Y. Xu, I. Belopolski, N. Alidoust, M. Neupane, G. Bian, C. Zhang, R. Sankar, G. Chang, Z. Yuan, C.-C. Lee, *et al.*, Discovery of a weyl fermion semimetal and topological fermi arcs, *Science* **349**, 613 (2015).

[3] B. Lv, H. Weng, B. Fu, X. P. Wang, H. Miao, J. Ma, P. Richard, X. Huang, L. Zhao, G. Chen, *et al.*, Experimental discovery of weyl semimetal taas, *Physical Review X* **5**, 031013 (2015).

[4] L. Lu, Z. Wang, D. Ye, L. Ran, L. Fu, J. D. Joannopoulos, and M. Soljačić, Experimental observation of weyl points, *Science* **349**, 622 (2015).

[5] H.-J. Kim, K.-S. Kim, J.-F. Wang, M. Sasaki, N. Satoh, A. Ohnishi, M. Kitaura, M. Yang, and L. Li, Dirac versus weyl fermions in topological insulators: Adler-bell-jackiw anomaly; format; in transport phenomena, *Physical review letters* **111**, 246603 (2013).

[6] S.-M. Huang, S.-Y. Xu, I. Belopolski, C.-C. Lee, G. Chang, B. Wang, N. Alidoust, G. Bian, M. Neupane, C. Zhang, *et al.*, A weyl fermion semimetal with surface fermi arcs in the transition metal monopnictide taas class, *Nature communications* **6**, 7373 (2015).

[7] S. Murakami, Phase transition between the quantum spin hall and insulator phases in 3d: emergence of a topological gapless phase, *New Journal of Physics* **9**, 356 (2007).

[8] X. Wan, A. M. Turner, A. Vishwanath, and S. Y. Savrasov, Topological semimetal and fermi-arc surface states in the electronic structure of pyrochlore iridates, *Physical Review B—Condensed Matter and Materials Physics* **83**, 205101 (2011).

[9] K.-Y. Yang, Y.-M. Lu, and Y. Ran, Quantum hall effects in a weyl semimetal: Possible application in pyrochlore iridates, *Physical Review B—Condensed Matter and Materials Physics* **84**, 075129 (2011).

[10] A. Burkov and L. Balents, Weyl semimetal in a topological insulator multilayer, *Physical review letters* **107**, 127205 (2011).

[11] G. Xu, H. Weng, Z. Wang, X. Dai, and Z. Fang, Chern semimetal and the quantized anomalous hall effect in hgcr 2 se 4, *Physical review letters* **107**, 186806 (2011).

[12] B. Lv, N. Xu, H. Weng, J. Ma, P. Richard, X. Huang, L. Zhao, G. Chen, C. Matt, F. Bisti, *et al.*, Observation of weyl nodes in taas, *Nature Physics* **11**, 724 (2015).

[13] H. B. Nielsen and M. Ninomiya, A no-go theorem for regularizing chiral fermions, *Physics Letters B* **105**, 219 (1981).

[14] S. Borisenko, D. Evtushinsky, Q. Gibson, A. Yaresko, K. Koepenik, T. Kim, M. Ali, J. van den Brink, M. Hoesch, A. Fedorov, *et al.*, Time-reversal symmetry breaking type-ii weyl state in ybmnb2, *Nature communications* **10**, 3424 (2019).

[15] X. Huang, L. Zhao, Y. Long, P. Wang, D. Chen, Z. Yang, H. Liang, M. Xue, H. Weng, Z. Fang, *et al.*, Observation of the chiral-anomaly-induced negative magnetoresistance in 3d weyl semimetal taas, *Physical Review X* **5**, 031023 (2015).

[16] A. C. Potter, I. Kimchi, and A. Vishwanath, Quantum oscillations from surface fermi arcs in weyl and dirac semimetals, *Nature communications* **5**, 5161 (2014).

[17] P. J. Moll, N. L. Nair, T. Helm, A. C. Potter, I. Kimchi, A. Vishwanath, and J. G. Analytis, Transport evidence for fermi-arc-mediated chirality transfer in the dirac semimetal cd3as2, *Nature* **535**, 266 (2016).

[18] A. A. Burkov, Chiral anomaly and transport in weyl metals, *Journal of Physics: Condensed Matter* **27**, 113201 (2015).

[19] A. Zyuzin and A. Burkov, Topological response in weyl semimetals and the chiral anomaly, *Physical Review B—Condensed Matter and Materials Physics* **86**, 115133 (2012).

[20] A. A. Zyuzin and R. P. Tiwari, Intrinsic anomalous hall effect in type-ii weyl semimetals, *JETP letters* **103**, 717 (2016).

[21] J. Steiner, A. Andreev, and D. Pesin, Anomalous hall effect in type-i weyl metals, *Physical review letters* **119**, 036601 (2017).

[22] A. A. Soluyanov, D. Gresch, Z. Wang, Q. Wu, M. Troyer, X. Dai, and B. A. Bernevig, Type-ii weyl semimetals, *Nature* **527**, 495 (2015).

[23] P. Li, Y. Wen, X. He, Q. Zhang, C. Xia, Z.-M. Yu, S. A. Yang, Z. Zhu, H. N. Alshareef, and X.-X. Zhang, Evidence for topological type-ii weyl semimetal wte2, *Nature communications* **8**, 2150 (2017).

[24] G. Autes, D. Gresch, M. Troyer, A. A. Soluyanov, and O. V. Yazyev, Robust type-ii weyl semimetal phase in transition metal diphosphides  $xp_{-2}(x= mo, w)$ , *arXiv preprint arXiv:1603.04624* (2016).

[25] J. Jiang, Z. Liu, Y. Sun, H. Yang, C. Rajamathi, Y. Qi, L. Yang, C. Chen, H. Peng, C. Hwang, *et al.*, Signature of type-ii weyl semimetal phase in mote2, *Nature communications* **8**, 13973 (2017).

[26] A. Pal, M. Chinotti, L. Degiorgi, W. J. Ren, and C. Petrovic, Optical properties of ybmnb2: A type ii weyl semimetal candidate, *Physica B: Condensed Matter* **536**, 64 (2018).

[27] M. Zhang, Z. Yang, and G. Wang, Coexistence of type-i and type-ii weyl points in the weyl-semimetal osc2, *The Journal of Physical Chemistry C* **122**, 3533 (2018).

[28] T.-R. Chang, S.-Y. Xu, G. Chang, C.-C. Lee, S.-M. Huang, B. Wang, G. Bian, H. Zheng, D. S. Sanchez, I. Bełopolski, *et al.*, Prediction of an arc-tunable weyl fermion metallic state in  $mo \times w1-x te2$ , *Nature communications* **7**, 10639 (2016).

[29] S.-Y. Xu, N. Alidoust, G. Chang, H. Lu, B. Singh, I. Bełopolski, D. S. Sanchez, X. Zhang, G. Bian, H. Zheng, *et al.*, Discovery of lorentz-violating type ii weyl fermions in laalge, *Science advances* **3**, e1603266 (2017).

[30] S. Saha and S. Tewari, Anomalous nernst effect in type-ii weyl semimetals, *The European Physical Journal B* **91**, 4 (2018).

[31] G. Sharma, P. Goswami, and S. Tewari, Chiral anomaly and longitudinal magnetotransport in type-ii weyl semimetals, *Physical Review B* **96**, 045112 (2017).

[32] S. Mukherjee and J. Carbotte, Anomalous dc hall response in noncentrosymmetric tilted weyl semimetals, *Journal of Physics: Condensed Matter* **30**, 115702 (2018).

[33] T. M. McCormick, R. C. McKay, and N. Trivedi, Semi-classical theory of anomalous transport in type-ii topological weyl semimetals, *Physical Review B* **96**, 235116 (2017).

[34] Y. Ferreiros, A. Zyuzin, and J. H. Bardarson, Anomalous nernst and thermal hall effects in tilted weyl semimetals, *arXiv preprint arXiv:1707.01444* (2017).

[35] M. V. Berry, Quantal phase factors accompanying adiabatic changes, *Proceedings of the Royal Society of London. A. Mathematical and Physical Sciences* **392**, 45 (1984).

[36] D. Xiao, M.-C. Chang, and Q. Niu, Berry phase effects on electronic properties, *Reviews of modern physics* **82**, 1959 (2010).

[37] H. B. Nielsen and M. Ninomiya, The adler-bell-jackiw anomaly and weyl fermions in a crystal, *Physics Letters B* **130**, 389 (1983).

[38] D. T. Son and N. Yamamoto, Berry curvature, triangle anomalies, and the chiral magnetic effect in fermi liquids, *Physical review letters* **109**, 181602 (2012).

[39] D. Son and B. Spivak, 88j4412s: Chiral anomaly and classical negative magnetoresistance of weyl metals. vol. 88, *Phys. Rev. B* , 104412 (2013).

[40] N. Sinitsyn, Semiclassical theories of the anomalous hall effect, *Journal of Physics: Condensed Matter* **20**, 023201 (2007).

[41] F. Haldane, Berry curvature on the fermi surface: Anomalous hall effect;? format?; as a topological fermi-liquid property, *Physical review letters* **93**, 206602 (2004).

[42] K. Landsteiner, Anomalous transport of weyl fermions in weyl semimetals, *Physical Review B* **89**, 075124 (2014).

[43] J. H. KIM, Anomalous transport in a weyl metal (The Israel Academy of Science and Humanities, 2022).

[44] P. Laurell, R. Lundgren, and G. Fiete, Thermoelectric properties of weyl and dirac semimetals, *Bulletin of the American Physical Society* **60** (2015).

[45] Y. Gao, S. A. Yang, and Q. Niu, Geometrical effects in orbital magnetic susceptibility, *Physical Review B* **91**, 214405 (2015).

[46] A. Burkov, Negative longitudinal magnetoresistance in dirac and weyl metals, *Physical Review B* **91**, 245157 (2015).

[47] Q. Chen and G. A. Fiete, Thermoelectric transport in double-weyl semimetals (2016).

[48] Y. Gao, S. A. Yang, and Q. Niu, Intrinsic relative magnetoconductivity of nonmagnetic metals, *Physical Review B* **95**, 165135 (2017).

[49] T. Morimoto, S. Zhong, J. Orenstein, and J. E. Moore, Semiclassical theory of nonlinear magneto-optical responses with applications to topological dirac/weyl semimetals, *Physical Review B* **94**, 245121 (2016).

[50] Y. Gao, Z.-Q. Zhang, H. Jiang, and K.-H. Ding, Suppression of magneto-optical transport in tilted weyl semimetals by orbital magnetic moment, *Physical Review B* **105**, 165307 (2022).

[51] K. Das and A. Agarwal, Linear magnetochiral transport in tilted type-i and type-ii weyl semimetals, *Physical Review B* **99**, 085405 (2019).

[52] R. Ghosh and I. Mandal, Direction-dependent conductivity in planar hall set-ups with tilted weyl/multi-weyl semimetals, *Journal of Physics: Condensed Matter* **36**, 275501 (2024).

[53] G. Sundaram and Q. Niu, Wave-packet dynamics in slowly perturbed crystals: Gradient corrections and berry-phase effects, *Physical Review B* **59**, 14915 (1999).

[54] S. Nandy, C. Zeng, and S. Tewari, Chiral anomaly induced nonlinear hall effect in semimetals with multiple

weyl points, Physical Review B **104**, 205124 (2021).

[55] D. Xiao, J. Shi, and Q. Niu, Berry phase correction to electron density of states in solids, Physical review letters **95**, 137204 (2005).

[56] E. Malic, T. Winzer, E. Bobkin, and A. Knorr, Microscopic theory of absorption and ultrafast many-particle kinetics in graphene, Physical Review B **84**, 205406 (2011).

[57] F. M. Pellegrino, M. I. Katsnelson, and M. Polini, Helicons in weyl semimetals, Physical Review B **92**, 201407 (2015).

[58] H. B. Nielsen and M. Ninomiya, Absence of neutrinos on a lattice:(i). proof by homotopy theory, Nuclear Physics B **185**, 20 (1981).

[59] A. Burkov, Giant planar hall effect in topological metals, Physical Review B **96**, 041110 (2017).

[60] S. Nandy, G. Sharma, A. Taraphder, and S. Tewari, Chiral anomaly as the origin of the planar hall effect in weyl semimetals, Physical review letters **119**, 176804 (2017).

[61] D. Ma, H. Jiang, H. Liu, and X. Xie, Planar hall effect in tilted weyl semimetals, Physical Review B **99**, 115121 (2019).

[62] N. Kumar, S. N. Guin, C. Felser, and C. Shekhar, Planar hall effect in the weyl semimetal gdptbi, Physical Review B **98**, 041103 (2018).

[63] J. Yang, W. Zhen, D. Liang, Y. Wang, X. Yan, S. Weng, J. Wang, W. Tong, L. Pi, W. Zhu, *et al.*, Current jetting distorted planar hall effect in a weyl semimetal with ultrahigh mobility, Physical Review Materials **3**, 014201 (2019).

[64] Y. Gao and B. Ge, Second harmonic generation in dirac/weyl semimetals with broken tilt inversion symmetry, Optics Express **29**, 6903 (2021).

[65] I. Sodemann and L. Fu, Quantum nonlinear hall effect induced by berry curvature dipole in time-reversal invariant materials, Physical review letters **115**, 216806 (2015).

[66] L. Wu, S. Patankar, T. Morimoto, N. L. Nair, E. Thewalt, A. Little, J. G. Analytis, J. E. Moore, and J. Orenstein, Giant anisotropic nonlinear optical response in transition metal monopnictide weyl semimetals, Nature Physics **13**, 350 (2017).

[67] C.-L. Zhang, T. Liang, Y. Kaneko, N. Nagaosa, and Y. Tokura, Giant berry curvature dipole density in a ferroelectric weyl semimetal, npj Quantum Materials **7**, 103 (2022).